2022

Optimal Allocation of Distributed Generation with the Presence of Photovoltaic and Battery Energy Storage System Using Improved Barnacles Mating Optimizer

Ali Selim

Faculty of Engineering, Aswan University, Egypt

Salah Kamel

Faculty of Engineering, Aswan University, Egypt

Hossam Zawbaa

Technological University Dublin, Ireland, hossam.Zawbaa@tudublin.ie

See next page for additional authors

Recommended Citation

Selim, A., Kamel, S. & Zawbaa, H.M. (2022). Optimal allocation of distributed generation with the presence of photovoltaic and battery energy storage system using improved barnacles mating optimizer. *Energy Science and Engineering*, vol. 10, no. 4. https://doi.org/10.1002/ese3.1182

Authors
Ali Selim, Salah Kamel, Hossam Zawbaa, Baseem Khan, and Francisco Jurado

Received: 8 January 2022 | Revised: 19 April 2022 | Accepted: 25 April 2022

DOI: 10.1002/ese3.1182

ORIGINAL ARTICLE

Optimal allocation of distributed generation with the presence of photovoltaic and battery energy storage system using improved barnacles mating optimizer

Ali Selim[1,2] | Salah Kamel[1] | Hossam M. Zawbaa[3,4] | Baseem Khan[5] | Francisco Jurado[2]

[1]Department of Electrical Engineering, Faculty of Engineering, Aswan University, Aswan, Egypt

[2]Department of Electrical Engineering, University of Jaén, EPS Linares, Jaén, Spain

[3]Faculty of Computers and Artificial Intelligence, Beni-Suef University, Beni-Suef, Egypt

[4]Technological University Dublin, Dublin, Ireland

[5]Department of Electrical Engineering, University, Hawassa, Ethiopia

Correspondence
Baseem Khan, Department of Electrical Engineering, Hawassa University, Ethiopia.
Email: baseem.khan04@gmail.com

Abstract

This paper proposes an improved version of Barnacles mating optimizer (BMO) for solving the optimal allocation problem of distribution generator (DGs) in radial distribution systems (RDSs). BMO is a recent bioinspired optimization algorithm that mimics the intelligence behavior of Barnacles' mating. However, like with any metaheuristic optimization approach, it may face issues such as local optima trapping and low convergence rate. Hence, an improved BMO is adopted based on the quasi oppositional (QOBMO) and the chaos maps theories (CQOBMO). The two improvement methods are applied to increase the convergence performance of the conventional BMO. To prove the efficiency of the improved QOBMO and CQOBMO algorithms, 23 benchmark functions are used, and the accomplished results are compared with the conventional BMO. Then, the improved algorithm is applied to minimize the total power and energy losses in the distribution systems considering the uncertainty of DG power generation and time-varying load demand. The uncertainty of DG is represented using photovoltaic-based DG (PVDG). The improved method is employed to find the optimal power scheduling of PVDG and battery energy storage (BES) during 24 h. Two standard IEEE RDS (IEEE 33-bus and IEEE 69-bus) are used to simulate the case studies. Finally, the obtained results show that significant loss reductions (LRs) are achieved using the improved BMO where LRs reach 65.26%, and 68.86% in IEEE 33-bus and 69-bus, respectively, in the case of PVDG integration. However, using PVDG and BES the energy loss reductions reach 64% and 67.80% in IEEE 33-bus and 69-bus, respectively, which prove the efficiency of the improved BMO algorithm in finding the optimal solutions obtained so far.

KEYWORDS

barnacles mating optimizer, chaos theories, DG placement, power losses reduction, quasi oppositional

1 | INTRODUCTION

1.1 | Distribution generator (DG) allocation problem

The rising interest in mitigating the effects of CO_2 emissions has prompted the power systems community to consider using clean renewable energy resources.[1] DGs are small generation units that are directly inserted into distribution networks at appropriate locations to maximize customer reliability.[2] Moreover, because of their capability to inject sufficient power at a strategic place, DGs played an essential role in decreasing power loss in the distribution system. However, based on different points of view, the potential large-scale penetration of DGs can result in both positive and negative consequences. Key negative effects include power flows, voltage levels, and power loss.[3] As a result, assessing these resources and their implications on electricity is critical. As a consequence, various efforts have been made in recent years to tackle the challenge of optimal DG distribution.

Furthermore, numerous studies have focused on sizing DG units based on load demand and generating electricity at specific times (snapshot or peak demand). Therefore, several variables have been neglected, particularly when integrating DG units that depend on renewable energy sources like photovoltaic base DG (PVDG). The generation levels of this type of DG are varied due to the intermittent nature of resources. The time-varying nature of load demand and the unpredictability of DG power output has been studied by a few studies.[4,5]

Two techniques have been used to deal with nondispatchable energy resources. The first one used power curtailment used in case of high generation or low demand, while the second used energy storage.[6] Because of its capacity to charge or discharge the appropriate energy during demand and generation variations, battery energy storage (BES) is regarded as more efficient than power curtailment.[7,8] Consequently, optimal scheduling of BES and PVDG is necessary to convert the non-dispatchable PVDG to a dispatchable power generation.

Consequently, optimization methods have been used in many types of research works to achieve the optimal allocation of the DG and BES into the distribution system.

1.2 | Overview of the optimization algorithms

Optimization can be defined as a procedure of accomplishing the most appropriate solutions for a combination of variables that achieve the objective of a problem in terms of maximization or minimization.[9] Recently, many optimization algorithms have been suggested to find the appropriate solutions to optimization problems. These optimization algorithms may be classified into several groups based on their nature, such as numerical approaches and stochastic algorithms.[10,11]

A mathematical model for the optimization issue should be used in the numerical-based approach. However, this technique requires certain gradient information to evaluate better solutions around the starting locations of the local search. Furthermore, it is more sensitive to the starting locations.[10]

On the other hand, stochastic algorithms have a random nature and may provide a different result each time.[11] The most common stochastic algorithm is the metaheuristic optimization method, which is distinguished by its simplicity and efficiency. Based on the source of inspiration, metaheuristic optimization algorithms are divided into four groups. These groups are; evolutionary, swarm, physics, and human behavior-based algorithms.[12,13]

In the first group (evolutionary-based algorithm), The nature of genetic evolution serves as the primary motivation. Where a generation of superior children inheriting the characteristics of the parents leads to the achievement of the global optimum. Hence, in this form, a method, mutation, selection, and crossover have been used. These are some good instances of these algorithms that have demonstrated their usefulness in optimization problems; DE,[14] genetic algorithms (GA),[15] Physarum inspired computational model (PCM),[16] human evolutionary model,[17] and biogeography based optimization.[18]

The social behavior of groupings of particles and animals inspires swarm-based algorithms. The intelligent behavior of the individual search agent in the swarm and the combination of these behaviors offer these kinds an advantage over other algorithms in achieving the global optima. The most widely used swarm algorithms are as follows: particle swarm optimization (PSO),[19] moth-flame optimization algorithm (MFO),[20] social spider optimization (SSO),[21] grey wolf optimizer (GWO),[22] artificial bee colony (ABC),[23] grasshoppers optimization algorithm (GOA),[24] border collie optimization (BCO),[11] whale optimization algorithm (WOA),[13] salp swarm algorithm (SSA),[25] Harris hawk optimization (HHO),[26] bear smell search algorithm BSSA,[27] bonobo optimizer (BO),[28] moth search algorithm (MSA),[29] hunger games search (HGS),[30] colony predation algorithm (CPA),[31] and monarch butterfly optimization (MBO).[32]

Physical-based algorithms exploit the occurrence of physical phenomena to execute the optimization paradigm, as follows: atom search optimization (ASO),[33] simulated annealings (SA),[34] water cycle algorithm (WCA),[35] gravitational search optimization algorithm (GSA),[36] water evaporation optimization (WEO),[37] lightning search algorithm (LSA),[38] equilibrium Optimizer (EO),[39] and artificial ecosystem-based optimization (AEO),[10] and slime mold algorithm (SMA).[40]

Human behavior-based algorithms, which replicate human social actions and beliefs, are the fourth type; examples of these algorithms are known as; the most valuable player algorithm (MVPA),[41] human-inspired algorithms (HIA),[42] teaching–learning-based optimization (TLBO),[43] social group optimization (SGO),[44] league championship algorithm (LCA),[45] and gaining-sharing knowledge (GSK).[46] However, some optimization algorithms have been implemented based on the metaphor such as the Runge–Kutta method (RUN),[47] Rao optimizer,[48] and others based on the weighted mean of vectors (INFO).[49]

1.3 | Improving the optimization algorithms

The power of meta-heuristic optimizations comes from their simplicity of implementation. Besides, they are more efficient in dealing with many optimization problems. However, based on the theorem of optimization called no-free-lunch,[50] which rises that no optimization algorithm can deal with all optimization problems and achieve the best results so far. Hence, many researchers tended to improve existing optimization algorithms or tried to develop new algorithms.

Various methods have been applied to improve the metaheuristic optimization algorithms. Chaos theory[51] has been widely utilized in metaheuristic algorithms to change their random parameters. Ten chaotic maps have been employed to enhance many optimization algorithms, achieving better results.[52] The application of chaos in GA has been introduced in Li-Jiang and Tian-Lun[53] and improved chaotic PSO proposed in Li et al.[54] Besides, the chaos theory has been used in the new optimization algorithms such as chaotic antlion optimization (CALO),[55] Chaotic whale optimization algorithm,[56] Chaotic grey wolf optimization algorithmCGWO,[57] chaotic biogeography-based optimizations (CBBO),[58] and recently in chaotic sine cosine algorithm (CSCA)[4] and CHHO.[59]

Also, opposition-based learning (OBL)[60] has been handled to improve metaheuristic optimization algorithms where the improvement can be accomplished using both the candidate solutions and their opposites at the same time, and then the best one will be applied for the next process. Some of the applications of OBL are in quasi-oppositional TLBO (QOTLBO),[61,62] and quasi-oppositional swine influenza model-based optimization with quarantine (QOSIMBO-Q),[63] and oppositional Jaya algorithm.[64]

Moreover, a multipopulation method has been proposed and applied to metaheuristic algorithms. The economic dispatch problem has been solved using a multipopulation Jaya algorithm in Lian et al.,[65] and Mingxue et al.,[66] and a multipopulation GA has been presented to control the adjustable hydraulic torque converter.

1.4 | Application of optimization algorithms in DG allocation

Optimization approaches have been utilized in a variety of research studies to obtain the best possible allocation of DG and BES into the distribution system.[67] The power system employed two main optimization algorithms: analytical algorithms and metaheuristic algorithms.[68]

To explore the impact of injected DG power on power system performance, a mathematical framework for the power system is completely defined in analytical algorithms as specified in the improved analytical (IA) and exhaustive load flow (ELF) optimization algorithms.[69] However, because of their dependence on the system topology, several of the analytical approaches are unsuitable for determining the appropriate size and position of numerous DGs.[70]

Therefore, some researchers shifted to optimization algorithms based on metaheuristics. The effectiveness of metaheuristic algorithms to solve optimization problems without going in-depth into the problem's complexity is a significant feature of their employment.

A GA, which optimizes the DG in the distribution system, has been used to minimize the total power consumption for a single objective problem.[71] To minimize the active power loss, the optimization of the particle swarm (PSO) has been implemented for the DG allocation, including various load models.[68,72] Optimization algorithms based on artificial intelligence have been used to evaluate the optimum location for multiple DGs in Hung and Colleagues.[69,73] An algorithm for fuzzy and clonal selection has been developed for DG allocation in Lalitha et al.[74] Recently, a variety of nature-inspired optimization algorithms were used in the DG allocation problem, such as the backtracking optimization algorithm (BSOA),[75] bacterial foraging optimization algorithm (BFOA),[76] stud krill herd algorithm (SKHA),[77] whale optimization algorithm (WOA),[78] and chaotic sine cosine (CSCA).[4]

1.5 | Contribution and paper organization

Based on the above literature, improvement of the metaheuristic optimization algorithms leads to achieving better results. Hence, in this paper, a new bioinspired barnacle mating optimizer (BMO) that belongs to evolutionary algorithms is improved using the OBL and chaos theories. BMO has been proposed in Sulaiman et al.,[9] and it mimics the mating process in the barnacles to produce new offspring. In the improved BMO, a quasi-oppositional of the new offspring is calculated and applied accompanied to the existing offspring in the primary objective function. The best one that gives the best objective function will be used in the next process. Besides, chaos maps are utilized to vary the exploration parameter of the BMO instead of using random values.

Hence, the main contributions of this paper can be summarized as follows:

- To study the impact of the intermittent nature of the PV power and the load variation on the performance of the radial distribution system (RDSs), an uncertainty model for PV power is formulated based on statistical data of the solar irradiance. In addition, to avoid the uncertainty of the PV power, BES is modeled to be optimally scheduled over 24 h.
- To enhance the optimization algorithms, improved versions of the original BMO optimization algorithms are proposed. Two improved methods are applied based on chaos and quasi oppositional theories.
- To check the efficiency of the improved BMO method, 23 benchmark functions are used and parametric and nonparametric statistical analyses are carried out.
- The improved BMO is used to allocate PVDG into standard IEEE 33-bus and IEEE 69-bus systems to minimize the total power loss.
- Finally, the improved optimization BMO algorithm is applied to allocate PV+BES into RDSs which leads to significant enhancements in the energy reduction and voltage profile.

The remainder of the paper is prepared as follows: Section 2 gives the mathematical formulation of the DG allocation problem; Section 3 presents an overview of the BMO algorithm; Section 4 presents the improved BMO based on the OBL and chaos maps. Section 5 demonstrates numerical results; Section 6 exhibits the conclusions.

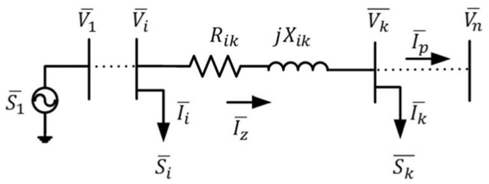

FIGURE 1 Single line diagram for radial distribution system.

2 | FORMULATION OF THE DG ALLOCATION PROBLEM

The goal of DG allocation in the power system is to reduce the total active power losses P_{loss}.

$$f = \min(P_{\text{loss}}). \tag{1}$$

Figure 1 exhibits a simple representation of the RDS where:

n is the number of buses. $\overline{S_1}$ and $\overline{V_1}$ are the complex power and the voltage at Bus 1. R_{ik} and X_{ik} are the resistance and reactance between Bus i and k. $\overline{I_i}$ and $\overline{I_k}$ are the load current at Bus i and k. $\overline{I_p}$ is the sum of current from Bus k to n.

To calculate the power losses a branch's current $|\overline{I_z}|$ (see Figure 1) and the branch resistance R_{ik} are used as[70]:

$$P_{\text{loss}} = \sum_{z=1}^{N_{\text{br}}} |\overline{I_z}|^2 R_{ik}, \tag{2}$$

where z is the branch number and N_{br} is the total number of branches

2.1 | Problem constraints

To optimally place the DG in the power system, some important constraints must be considered, such as equality and inequality.

(1) Equality constraints

The generation power P_{g_i} by NG number of DG should not exceed the power loss and the load demand P_d:

$$\sum_{i=1}^{\text{NG}} P_{g_i} = P_{\text{loss}} + P_d, \tag{3}$$

where the number of installed DG is represented by NG

(2) Inequality constraints
The inequality constraints are very important for the operation of the power system; hence, these boundaries should be considered as:

(a) *Active power generation limits*

$$P_{g_i}{}^{\min} \le P_{g_i} \le P_{g_i}{}^{\max}. \tag{4}$$

(b) *Reactive power generation limits*

$$Q_{g_i}{}^{\min} \le Q_{g_i} \le Q_{g_i}{}^{\max}. \tag{5}$$

(c) *Limits of the bus voltage*

$$0.95 \le V_i \le 1.05. \tag{6}$$

2.2 | PVDG power generation

To model the intermittent nature of the PV power during 24 h, probability distribution functions (PDF) are used.[79] Based on historical data, a typical day of solar irradiance can be generated. The output power of the PV can be implemented using beta PDF as follows:

(1) Modelling of solar irradiance
In this model, beta PDF is employed to formulate the probabilistic nature of solar irradiance s^t (kW/m^2) at each time t as follows:

$$f_b(s^t) = \begin{cases} \frac{\Gamma(\alpha^t+\beta^t)}{\Gamma\alpha^t+\Gamma\beta^t} \quad (s^t)^{\alpha^t-1}(1-s^t)^{\beta^t-1} & \begin{matrix} 0 \le s^t \le 1 \\ \alpha^t, \beta^t > 0 \end{matrix} \\ 0 & \text{otherwise} \end{cases} \tag{7}$$

where α^t and β^t are the beta PDF parameters and their values are computed with the mean μ_s^t and the standard deviation σ_s^t of the solar irradiance as:

$$\beta^t = \left(1-\mu_s^t\right)\left(\frac{\left(1+\mu_s^t\right)\mu_s^t}{\left(\sigma_s^t\right)^2}\right), \tag{8}$$

$$\alpha^t = \frac{\mu_s^t * \beta^t}{\left(1-\mu_s^t\right)}. \tag{9}$$

(2) Power generation of PV

The average power P_{PV}^t of the PV array at time t is calculated as follows:

$$P_{\mathrm{PV}}^t = \sum_{i=1}^{n_s} P_o\left(s_i^t\right) f_b\left(s_i^t\right), \tag{10}$$

where $P_o(s^t)$ is the output power of the PV module and can be computed as[79]:

$$P_o(s^t) = N_m \times V_c \times I_c \quad \left(\frac{V_{\mathrm{MPP}} \times I_{\mathrm{MPP}}}{V_o \times I_s}\right), \tag{11}$$

where N_m is the modules' number of the PV, V_{MPP} and I_{MPP} the maximum power point voltage and current, respectively, V_o is the open-circuit voltage and I_s is the short circuit current, and V_c, I_c are the cell voltage and current, respectively, and they can be calculated using the following equations:

$$V_c = V_o - K_v \times T_c, \tag{12}$$

$$I_c = s^t\left(I_s + K_i(T_c - 25)\right), \tag{13}$$

where K_v, K_i are the voltage and current temperature coefficient (V/°C), (A/°C), respectively, T_c is the cell temperature (°C), and it can be determined as:

$$T_c = T_A + s^t\left(\frac{T_0 - 20}{0.8}\right). \tag{14}$$

where T_A is the ambient temperature and T_0 is the nominal operating temperature.

In this study, 3 years of data on the solar irradiance are used as given in Hung et al.,[80] and the beta PDF of the solar irradiance is calculated and drawn as shown in Figures 2 and 3.

2.3 | PVDG and BES power model

The main problem with the integration of PVDG is its intermittent nature and availability for 24 h. Hence, to avoid these problems, the charging/discharging of BES can be used with the PVDG. The mathematical formulation of the daily energy charging $(E_{\mathrm{BES}_i})_c$ and discharging $(E_{\mathrm{BES}_i})_d$ at the bus, i are obtained as:

$$(E_{\mathrm{BES}_i})_c = \sum_{t=1}^{24} (P_{\mathrm{BES}_i}^t)_c \times \Delta t, \tag{15}$$

$$(E_{\mathrm{BES}_i})_d = \sum_{t=1}^{24} (P_{\mathrm{BES}_i}^t)_d \times \Delta t, \tag{16}$$

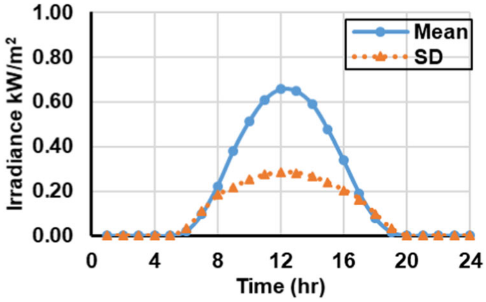

FIGURE 2 The mean and standard deviation of the solar irradiance.

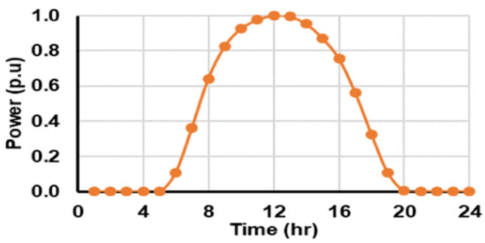

FIGURE 3 Photovoltaic output power generation per unit.

where $(P^t_{\mathrm{BES}_i})_c$ and $(P^t_{\mathrm{BES}_i})_d$ are the charge and discharge power of the BES, respectively. The PV + BES system has two output energies based on the BES status (either charge or discharge), as shown in Figure 4. Hence, the total output energy $E_{(\mathrm{PV+BES})_i}$ in case of discharging can be expressed as:

$$E_{(\mathrm{PV+BES})_i} = (E_{\mathrm{BES}_i})_d + (E_{\mathrm{PV}_i})_G, \tag{17}$$

where $(E_{\mathrm{PV}_i})_G$ is the energy of PV, which is injected into the grid at bus i.

On the other hand, the energy of the PV unit at bus i which is named E_{PV_i} in the case of BES charging is:

$$E_{\mathrm{PV}_i} = (E_{\mathrm{BES}_i})_c + (E_{\mathrm{PV}_i})_G. \tag{18}$$

The relation between the charging and discharging energies of the BES can be expressed using the roundtrip efficiency ($\eta_B = \eta_d * \eta_c$) as:

$$(E_{\mathrm{BES}_i})_d = \eta_B (E_{\mathrm{BES}_i})_c. \tag{19}$$

To find the E_{PV_i} of the PV generation, Equations (17) and (18) are reformulated as:

$$E_{\mathrm{PV}_i} = \frac{E_{(\mathrm{PV+BES})_i} - (1-\eta_B)(E_{\mathrm{PV}_i})_G}{\eta_B} \tag{20}$$

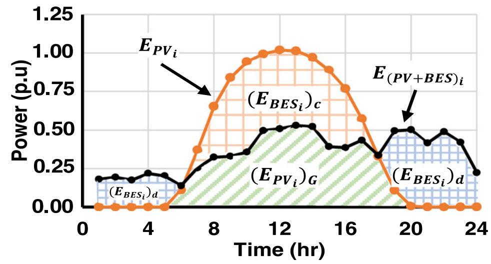

FIGURE 4 PV + BES output power generation per unit. BES, battery energy storage; PV, photovoltaic.

After obtaining the E_{PV_i}, the maximum power of the PV unit can be calculated using the capacity factor of the PV module (C^U_{PV}) as follows:

$$P_{\mathrm{PV}_i} = C^U_{\mathrm{PV}} E_{\mathrm{PV}_i} \tag{21}$$

where

$$C^U_{\mathrm{PV}} = \frac{P^U_{\mathrm{PV}}}{E^U_{\mathrm{PV}}}, \tag{22}$$

P^U_{PV} is the maximum output of a PV module unit, and E^U_{PV} is the energy of PV that is generated over a 24-h day.

According to Equations (20) and (21), the required power of the PVDG can be expressed in the following equation:

$$P_{\mathrm{PV}_i} = C^U_{\mathrm{PV}} \left(\frac{E_{(\mathrm{PV+BES})_i} - (1-\eta_B)(E_{\mathrm{PV}_i})_G}{\eta_B} \right). \tag{23}$$

3 | OVERVIEW OF BMO

The structure of the BMO algorithm involves three main steps that start with the initialization of the barnacles, then the mating process, and finally, the reproduction of the offspring.[9] These steps are mathematically implemented in the next sections.

3.1 | Initialization of the barnacles

In the BMO, barnacles are randomly initialized based on control variables number N and the number of barnacles n as follows:

$$X = \begin{bmatrix} x_1^1 \cdots x_1^N \\ \vdots \quad \ddots \quad \vdots \\ x_n^1 \cdots x_n^N \end{bmatrix} \tag{24}$$

where the barnacles X should be within the boundary limits as:

$$X_{\mathrm{lb}} \le X \le X_{\mathrm{ub}}, \tag{25}$$

where X_{lb} and X_{ub} are the lower and upper vector bounds, respectively, and can be expressed as:

$$\begin{aligned} X_{\mathrm{lb}} &= \left[x_{\mathrm{lb}}^{1}, \ldots, x_{\mathrm{lb}}^{N}\right], \\ X_{\mathrm{ub}} &= \left[x_{\mathrm{ub}}^{1}, \ldots, x_{\mathrm{ub}}^{N}\right]. \end{aligned} \tag{26}$$

3.2 | Mating process

In real life, each barnacle can inject its sperm as well as absorb it from other barnacles. Hence, three mating scenarios can occur. These scenarios are named normal mating, self-mating, and sperm cast mating. However, as assumed in the BMO algorithm,[9] the mating process occurs only between two barnacles. Hence, self-mating is not considered in BMO.

On the one hand, normal mating (exploitation) occurs when the absolute distance between two barnacles is less than the penis length *pl* that has been set. On the other hand, the sperm cast (exploration) happens when the absolute distance is more than *pl*.

The mathematical formulation of this behavior can be achieved by forming two vectors of parents' IDs from the overall barnacles' population as follows:

$$\begin{aligned} ID_D &= randperm(N) \\ ID_M &= randperm(N) \end{aligned} \tag{27}$$

where ID_D and ID_M are vectors of identification numbers of Dads and Mums, respectively. *randperm* is a function that returns a vector including a random variation of the integers 1 to N.

3.3 | Reproduction process

The reproduction of the new offspring in the BMO has been achieved based on the mating scenario in a simple formulation. For normal mating, the latest offspring can be expressed as:

$$x_i^{\mathrm{N\_new}} = \alpha x_{ID_D}^{N} + \beta x_{ID_M}^{N}, \tag{28}$$

where α is a random number between [0,1], $\beta = (1 - \alpha)$, $x_{\mathrm{ID_D}}^{N}$, and $x_{\mathrm{ID_M}}^{N}$ are the Dad and Mum variables of the selected barnacles.

On the other hand, if the barnacles exceed the range of *pl* then the sperm cast should occur as follows:

$$x_i^{\mathrm{N\_new}} = \gamma x_{\mathrm{ID_M}}^{N}, \tag{29}$$

where γ is a random variable between [0,1], it can be noticed that the Mum generates the new offspring, and thus, the Mum receives the sperm from the water injected by other barnacles elsewhere.

The overall description of the BMO algorithm is shown in Figure 5.

4 | IMPROVED BMO

As discussed in Section 1, different methods have been applied to improve the metaheuristic optimization algorithms. Therefore, quasi oppositional and chaos maps are handled to improve the performance of conventional BMO.

4.1 | Chaos maps

The second improvement in the BMO is using chaos theory based on several chaotic maps to enhance the exploration. Where chaotic maps are used to improve the convergence by applying the chaotic equation instead of utilizing random parameters Thus, 10 chaotic maps are adopted (see Table 1) and applied to the BMO and named CBMO algorithms to update the exploration parameter α instead of using random probability as follows:

$$\alpha = y_{\mathrm{iter}+1}, \tag{32}$$

where $y_{\mathrm{iter}+1}$ is the selected chaos map as presented in Table 1.

4.2 | Quasi oppositional

In this study, the opposite solutions of the BMO barnacles $X_i^{\mathrm{N\_new}}$ can be expressed as:

$$X_i^{\mathrm{QN\_new}} = \begin{cases} C + r_1\left(C - X_i^{\mathrm{N\_new}}\right), & X_i^{\mathrm{N\_new}} < C \\ C - r_1\left(X_i^{\mathrm{N\_new}} - C\right), & X_i^{\mathrm{N\_new}} \ge C \end{cases} \tag{30}$$

Where $X_i^{\mathrm{QN\_new}}$ is quasi oppositional of the $X_i^{\mathrm{N\_new}}$ barnacle and C are calculated as:

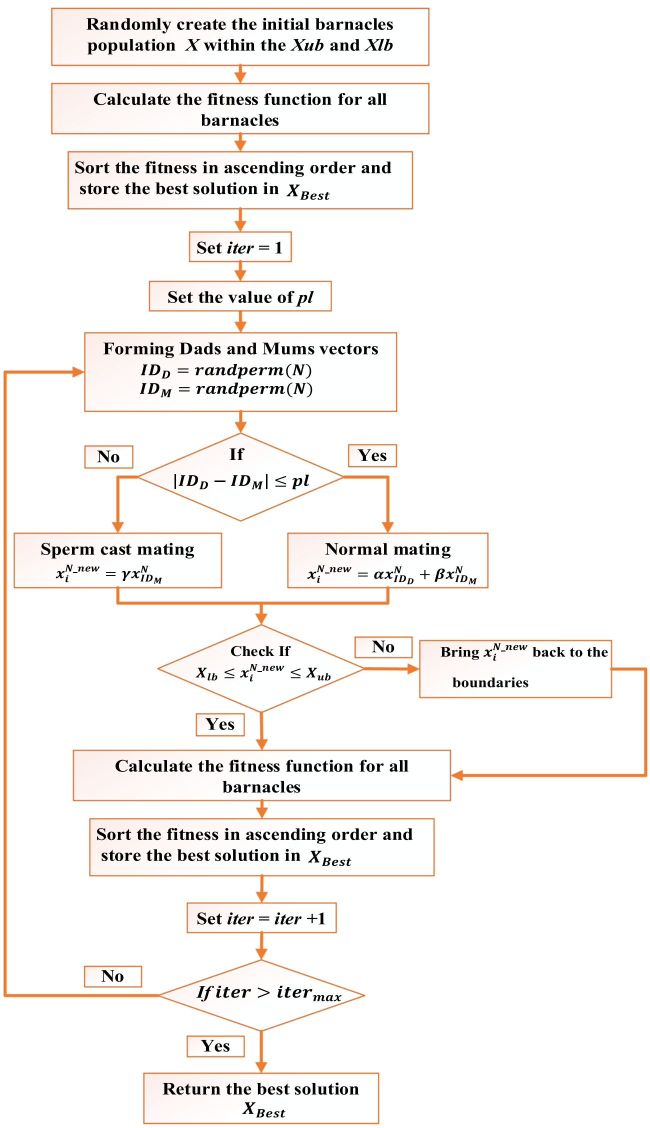

FIGURE 5 Barnacles mating optimizer algorithm.

$$C = \frac{x_{\mathrm{lb}}^i + x_{\mathrm{ub}}^i}{2}. \tag{31}$$

Hence $X_i^{\mathrm{N\_new}}$ and $X_i^{\mathrm{QN\_new}}$ are used to calculate the objective function, then the one who achieves the best objective is used in the next iterative process.

The overall steps of the QOBMO based on the quasi oppositional method are presented in Figure 6.

The chaotic maps and quasi oppositional are applied to the BMO to formulate CQOBMO. Hence, the overall steps of the CQOBMO are exhibited in the flowchart and shown in Figure 7.

Algorithm 1 presents a pseudo-code of the CQOBMO algorithm which explains the process of fusion of quasi oppositional and chaos maps by the BMO algorithm,

Algorithm 1. *CQOBMO formulation.*

```
Initialize a set of random barnacles X_i = (X_1, X_2, ..., X_n, ) within the limits X_lb ≤ X_i ≤ X_ub.
Calculate the objective function for each search barnacle.
Sort the fitness in ascending order and store the best solution in X_Best
Set the value of pl
while (iter < iter_max)
Update the selected chaotic map parameter y_iter
    Form two vectors of parents' IDs using (27)
    Using the chaotic y_iter, update the parameters, α using (32)
    for each search agent X_i
        if |ID_D − ID_M| ≤ pl
            Generate a new offspring using (28)
        else
            Generate a new offspring using (29)
        end if
  Calculate the quasi oppositional for all new barnacles using (30)
  Calculate the objective function.
  Sort the fitness in ascending order and update the best solution X_Best
  iter = iter + 1
end while
return the final best solution stored X_Best
```

5 | RESULT AND DISCUSSION

5.1 | Performance of the improved BMO

The performance of the improved BMO based on the quasi oppositional and chaotic maps is tested in this section using 23 benchmark functions.[22] These benchmarks have been divided into three main groups. The first group is unimodal, which includes the functions (F1–F7) and is characterized by one global optima solution; hence, they have been used to test the exploitation phase. The second and the third groups (F8–F14) are multimodal and composite (F15–F23), respectively, which test the algorithm's exploration phase.

In Sulaiman et al.,[9] the conventional BMO proved its effectiveness compared to many metaheuristic algorithms such as GA, PSO, ALO, MFO, WOA, GOA, SSA, and SCA. Hence, in this study, a comparison between BMO, 10 CBMOs, QOBMO, and 10 CQOBMOs

TABLE 1 The mathematical formulation of the chaotic maps.

No	Name	Chaotic map equation
1	Chebyshev	$y_{iter+1} = \cos(\text{iter} \times \cos^{-1}(y_{iter}))$
2	Circle	$y_{iter+1} = \text{mod}\left(y_{iter} + b_1 - \left(\frac{b_2}{2\pi}\right)\sin(2\pi y_{iter}), 1\right)$ $b_1 = 0.5$, $b_2 = 0.2$
3	Gauss/mouse	$y_{iter+1} = \begin{cases} 1, & y_{iter} = 0 \\ \frac{1}{\text{mod}(y_{iter})}, & \text{Otherwise} \end{cases}$
4	Iterative	$y_{iter+1} = \sin\left(\frac{b\pi}{y_{iter}}\right), b = 0.7$
5	Logistic	$y_{iter+1} = b y_{iter}(1 - y_{iter}), b = 4$
6	Piecewise	$y_{iter+1} = \begin{cases} \frac{y_{iter}}{H}, & 0 \le y_{iter} \le H \\ \frac{y_{iter} - H}{0.5 - H}, & H \le y_{iter} \le 0.5 \\ \frac{1 - H - y_{iter}}{0.5 - H}, & 0.5 \le y_{iter} \le 1 - H \\ \frac{1 - y_{iter}}{H}, & 1 - H \le y_{iter} \le 1 \end{cases}, H = 0.4$
7	Sine	$y_{iter+1} = \frac{b}{4}\sin(\pi y_{iter}), \quad b = 4$
8	Singer	$y_{iter+1} = u(7.86 y_{iter}^1 - 23.31 y_{iter}^{12} - 28.75 y_{iter}^3 - 13.302875 y_{iter}^4), u = 1.07$
9	Sinusoidal	$y_{iter+1} = b y_{iter}^1 \sin(\pi y_{iter}), b = 2.3$
10	Tent	$y_{iter+1} = \begin{cases} \frac{y_{iter}}{0.7}, & y_{iter} < 0.7 \\ \frac{10}{3}(1 - y_{iter}), & y_{iter} \ge 0.7 \end{cases}$

algorithms is presented to check the performance of the improved methods.

Statistical analysis is performed based on the average, worst, and best values for each benchmark function at 30 runs for each algorithm with 200 iterations and 30 barnacles. In addition, Wilcoxon signed-rank test (WSRT) is used as a nonparametric statistical test.

(1) First group benchmarks
As mentioned earlier, the first group of the benchmarks is unimodal, which has one global optimum. The numerical results of this group are summarized in Tables 2 and 3 for the improved CBMO and CQOBMO methods. The improved method QOBMO gives better results for all benchmark functions than the conventional BMO and CBMOs algorithms which proves the efficiency of the QOBMO. However, incorporating the chaotic maps into the BMO (CBMO_1, CBMO_2, etc., based on the chaotic map number) improve the obtained results as presented in Table 2. The results in Table 2 show that CBMO_7 gives the best results compared to the conventional and the other chaotic maps in F1, F2, F4, and F7. However, applying the chaotic maps and quasi oppositional to BMO gives the best results so far as presented in Table 3 and noticed in F2, F4, and F5 using CQOBMO_10, CQOBMO_7, and CQOBMO_9, respectively. Also, the improvement in the convergence characteristic is shown in Figure 7 for F1 and F2. Where all improved methods reach a better performance than the conventional BMO and the best-recorded methods are CQOBMO_1, and CQOBMO_10 in F1 and F2, respectively.

(2) Second group benchmarks
This group is characterized by its multiple local solutions, which leads the optimization algorithms to fall in them, as exhibited in Figure 8 (see F9 and F10). However, the improved methods still accomplish the best and are almost the same as the conventional BMO, as clear in Tables 4 and 5, unless the improved methods using the chaotic maps and quasi oppositional obtain the optimal solution in less iteration, as presented in Figure 8. Thus, the best objective function of F9 is obtained by the CQOBMO_3 in five iterations. For F10, the CQOBMO_10 reaches the minimum objective value in fourteen iterations, which is less than the conventional BMO and the QOBMO.

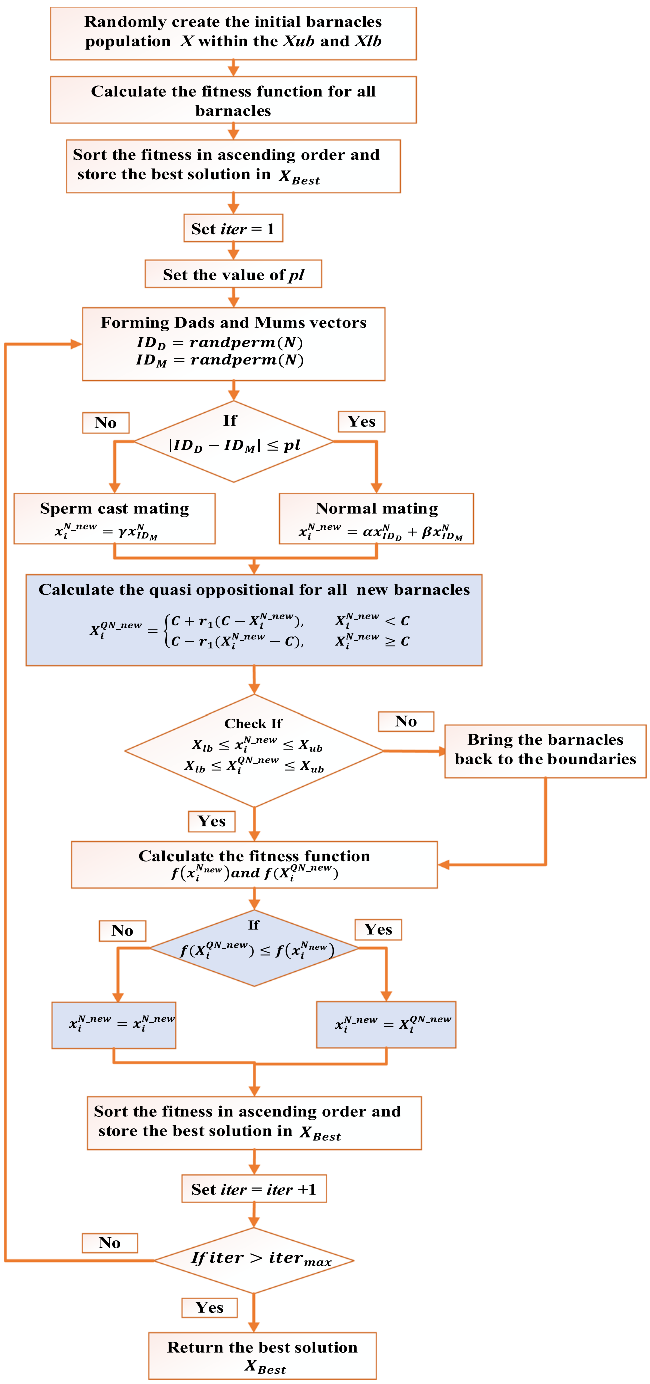

FIGURE 6 QOBMO algorithm.

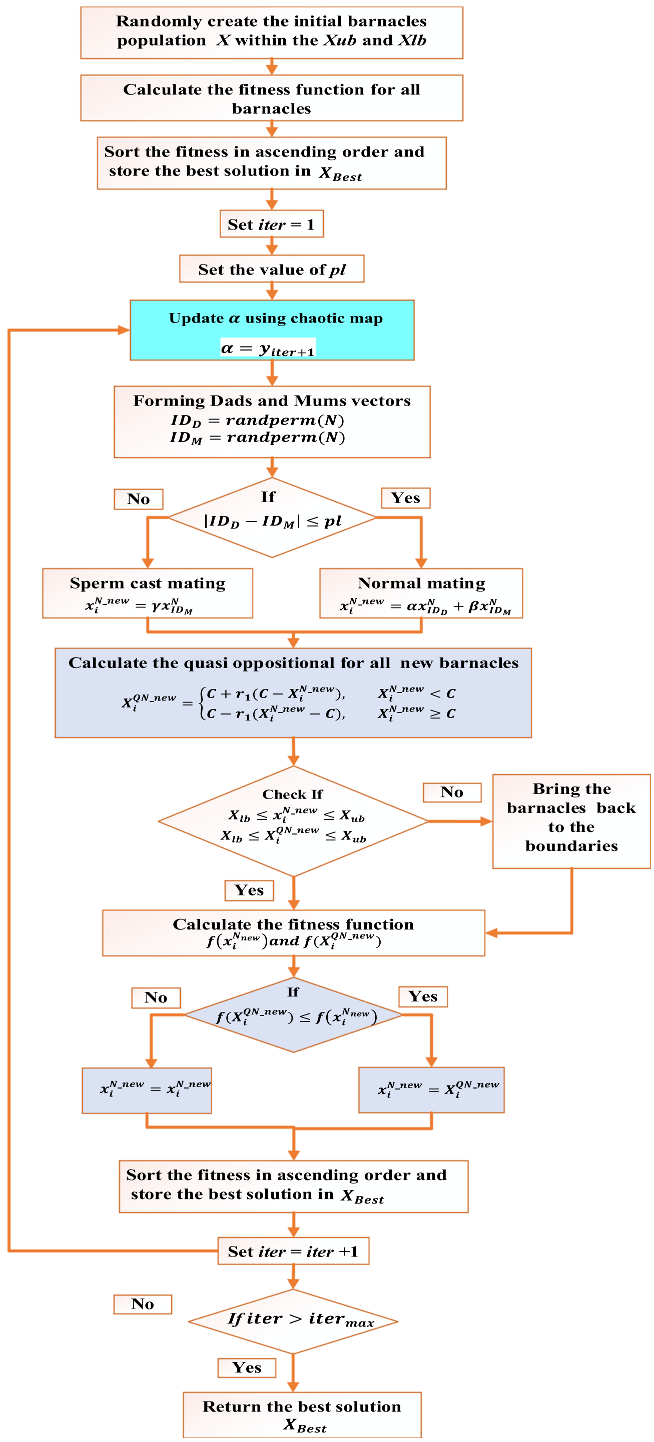

FIGURE 7 Flowchart of the CQOBMO algorithm.

(3) Third group benchmarks

This group was established by combining many real search spaces and different test functions, introducing challenging examinations for the optimization algorithms. Hence, the optimization suitable should be more stable and have an excellent balance between the exploration and exploitation phases to pass this test. Tables 6 and 7 give the obtained results of all algorithms applied to this group. The tables prove that the QOBMO gives the best solutions obtained so far besides the improved chaotic versions. The convergence characteristics (see Figure 8 for F15 and F16) illustrate that the CQOBMO_5 and CQOBMO_4 attain the best solutions obtained so far in F15 and F16, respectively.

From this analysis, the improved QOBMO and CQOBMO prove their ability to achieve the optimal

TABLE 2 Statistical analysis for the first group of the benchmarks (F1–F7) using Choatic maps.

		BMO	CBMO _1	CBMO _2	CBMO _3	CBMO _4	CBMO _5	CBMO _6	CBMO _7	CBMO _8	CBMO _9	CBMO _10
F1	Best	8.95E-252	1.93E-255	5.86E-262	3.53E-255	5.57E-253	1.42E-256	7.25E-255	**1.32E-264**	3.13E-255	1.78E-249	1.57E-249
	Avg	1.30E-220	2.56E-227	1.72E-221	7.82E-221	2.71E-225	2.15E-220	1.43E-228	**2.15E-229**	2.27E-223	3.02E-221	1.07E-222
	worst	2.77E-219	5.74E-226	3.01E-220	2.34E-219	8.06E-224	6.36E-219	2.56E-227	**5.50E-228**	6.81E-222	9.06E-220	2.16E-221
F2	Best	5.66E-125	7.25E-129	2.69E-124	2.32E-127	7.60E-128	3.05E-126	3.55E-128	**1.13E-132**	1.55E-130	2.46E-128	6.44E-129
	Avg	1.85E-110	1.15E-112	7.00E-114	6.36E-115	6.51E-114	7.35E-112	3.05E-114	**4.96E-116**	2.47E-111	1.57E-112	1.43E-110
	worst	5.45E-109	2.62E-111	2.05E-112	9.97E-114	1.31E-112	1.49E-110	6.51E-113	**7.81E-115**	7.39E-110	4.39E-111	4.23E-109
F3	Best	4.49E-256	1.67E-253	6.74E-257	**2.38E-267**	3.41E-261	1.60E-249	1.08E-254	2.97E-249	2.22E-257	2.78E-251	1.40E-264
	Avg	9.73E-213	6.18E-218	1.21E-220	4.11E-217	8.88E-225	2.96E-220	2.98E-223	7.01E-220	4.41E-224	1.61E-224	**1.72E-229**
	worst	2.92E-211	1.85E-216	3.63E-219	1.23E-215	2.61E-223	6.84E-219	8.92E-222	2.10E-218	1.05E-222	2.71E-223	**4.13E-228**
F4	Best	1.63E-127	2.37E-129	2.12E-125	2.30E-130	1.67E-128	3.55E-131	4.41E-130	**5.61E-132**	2.13E-127	1.96E-127	2.81E-129
	Avg	1.99E-110	1.54E-111	2.63E-111	1.93E-114	1.18E-111	3.57E-114	7.38E-114	**3.00E-116**	2.82E-114	1.38E-111	2.38E-114
	worst	5.85E-109	4.59E-110	7.89E-110	4.48E-113	3.55E-110	6.50E-113	1.27E-112	**8.75E-115**	6.05E-113	2.58E-110	6.43E-113
F5	Best	**2.77E+01**	2.89E+01	2.89E+01	2.89E+01	2.89E+01	2.89E+01	2.89E+01	2.89E+01	2.89E+01	2.89E+01	2.89E+01
	Avg	2.84E+01	2.90E+01	2.90E+01	2.90E+01	2.90E+01	2.90E+01	2.90E+01	2.90E+01	2.90E+01	2.90E+01	2.90E+01
	worst	2.88E+01	2.90E+01	2.90E+01	2.90E+01	2.90E+01	2.90E+01	2.90E+01	2.90E+01	2.90E+01	2.90E+01	2.90E+01
F6	Best	1.04E+00	4.53E+00	5.41E+00	5.09E+00	5.43E+00	5.56E+00	6.07E+00	5.11E+00	4.08E+00	5.49E+00	6.21E+00
	Avg	1.72E+00	6.92E+00	6.83E+00	6.83E+00	6.84E+00	6.93E+00	6.95E+00	6.77E+00	6.67E+00	6.86E+00	7.08E+00
	worst	2.26E+00	7.50E+00	7.50E+00	7.50E+00	7.50E+00	7.48E+00	7.50E+00	7.50E+00	7.33E+00	7.50E+00	7.50E+00
F7	Best	1.81E-06	3.73E-06	1.42E-06	9.62E-06	4.90E-06	2.25E-06	6.82E-06	**2.39E-08**	2.88E-06	1.12E-06	2.92E-08
	Avg	8.74E-05	7.24E-05	8.61E-05	8.49E-05	1.05E-04	7.30E-05	9.68E-05	**5.90E-05**	8.80E-05	9.18E-05	7.67E-05
	worst	3.70E-04	2.51E-04	4.03E-04	2.98E-04	4.60E-04	3.12E-04	3.54E-04	**2.03E-04**	4.96E-04	3.35E-04	2.28E-04

TABLE 3 Statistical analysis for the first group of the benchmarks (F1-F7) using chaotic maps and quasi oppostional.

		BMO	QOBMO	CQOBMO _1	CQOBMO _2	CQOBMO _3	CQOBMO _4	CQOBMO _5	CQOBMO _6	CQOBMO _7	CQOBMO _8	CQOBMO _9	CQOBMO _10
F1	Best	8.95E-252	**0.00E+00**	**0.00E+00**	**0.00E+00**	**0.00E+00**	**0.00E+00**	**0.00E+00**	**0.00E+00**	**0.00E+00**	**0.00E+00**	**0.00E+00**	**0.00E+00**
	Avg	1.30E-220	**0.00E+00**	**0.00E+00**	**0.00E+00**	**0.00E+00**	**0.00E+00**	**0.00E+00**	**0.00E+00**	**0.00E+00**	**0.00E+00**	**0.00E+00**	**0.00E+00**
	worst	2.77E-219	**0.00E+00**	**0.00E+00**	**0.00E+00**	**0.00E+00**	**0.00E+00**	**0.00E+00**	**0.00E+00**	**0.00E+00**	**0.00E+00**	**0.00E+00**	**0.00E+00**
F2	Best	5.66E-125	5.62E-250	2.27E-267	5.31E-266	4.07E-264	4.33E-265	1.56E-264	5.83E-267	2.54E-263	1.21E-267	1.79E-269	**9.42E-273**
	Avg	1.85E-110	1.96E-230	8.12E-236	1.27E-244	4.29E-237	5.84E-241	8.88E-241	**1.71E-248**	3.88E-242	3.96E-240	1.62E-246	5.15E-247
	worst	5.45E-109	5.88E-229	2.35E-234	3.79E-243	1.28E-235	1.65E-239	2.65E-239	**3.20E-247**	1.16E-240	1.18E-238	4.70E-245	1.55E-245
F3	Best	4.49E-256	**0.00E+00**	**0.00E+00**	**0.00E+00**	**0.00E+00**	**0.00E+00**	**0.00E+00**	**0.00E+00**	**0.00E+00**	**0.00E+00**	**0.00E+00**	**0.00E+00**
	Avg	9.73E-213	**0.00E+00**	**0.00E+00**	**0.00E+00**	**0.00E+00**	**0.00E+00**	**0.00E+00**	**0.00E+00**	**0.00E+00**	**0.00E+00**	**0.00E+00**	**0.00E+00**
	worst	2.92E-211	**0.00E+00**	**0.00E+00**	**0.00E+00**	**0.00E+00**	**0.00E+00**	**0.00E+00**	**0.00E+00**	**0.00E+00**	**0.00E+00**	**0.00E+00**	**0.00E+00**
F4	Best	1.63E-127	1.75E-257	3.04E-264	1.66E-270	8.34E-261	5.89E-271	8.08E-265	8.14E-267	**1.67E-275**	1.62E-264	5.23E-273	2.69E-267
	Avg	1.99E-110	5.55E-230	3.95E-244	3.06E-243	3.37E-237	7.73E-242	2.88E-238	2.13E-246	4.78E-236	**6.41E-247**	3.34E-244	1.51E-243
	worst	5.85E-109	1.67E-228	1.08E-242	9.19E-242	1.01E-235	2.32E-240	8.63E-237	5.78E-245	1.43E-234	**1.47E-245**	1.00E-242	4.52E-242
F5	Best	**2.77E+01**	2.79E+01	2.89E+01	2.89E+01	2.89E+01	2.89E+01	2.89E+01	2.89E+01	2.89E+01	2.89E+01	2.89E+01	2.89E+01
	Avg	2.84E+01	**2.83E+01**	2.90E+01	2.90E+01	2.90E+01	2.90E+01	2.90E+01	2.90E+01	2.90E+01	2.90E+01	2.90E+01	2.90E+01
	worst	2.88E+01	**2.88E+01**	2.90E+01	2.90E+01	2.90E+01	2.90E+01	2.90E+01	2.90E+01	2.90E+01	2.90E+01	2.90E+01	2.90E+01
F6	Best	1.04E+00	**9.40E-01**	4.24E+00	4.68E+00	5.34E+00	5.31E+00	4.76E+00	5.37E+00	4.91E+00	5.07E+00	4.68E+00	4.79E+00
	Avg	1.72E+00	**1.47E+00**	6.38E+00	6.28E+00	6.64E+00	6.56E+00	6.42E+00	6.59E+00	6.51E+00	6.50E+00	6.45E+00	6.44E+00
	worst	2.26E+00	**2.15E+00**	7.25E+00	7.36E+00	7.45E+00	7.37E+00	7.40E+00	7.31E+00	7.05E+00	7.45E+00	7.24E+00	7.29E+00
F7	Best	1.81E-06	1.52E-06	1.11E-06	4.52E-07	1.51E-07	9.24E-07	1.38E-06	2.37E-06	6.75E-07	1.59E-06	**1.64E-09**	7.47E-07
	Avg	8.74E-05	4.10E-05	4.03E-05	5.05E-05	5.82E-05	3.63E-05	4.49E-05	5.95E-05	3.65E-05	**3.60E-05**	4.06E-05	4.03E-05
	worst	3.70E-04	2.64E-04	1.94E-04	1.54E-04	3.24E-04	1.54E-04	1.71E-04	1.86E-04	**1.19E-04**	1.31E-04	1.46E-04	2.36E-04

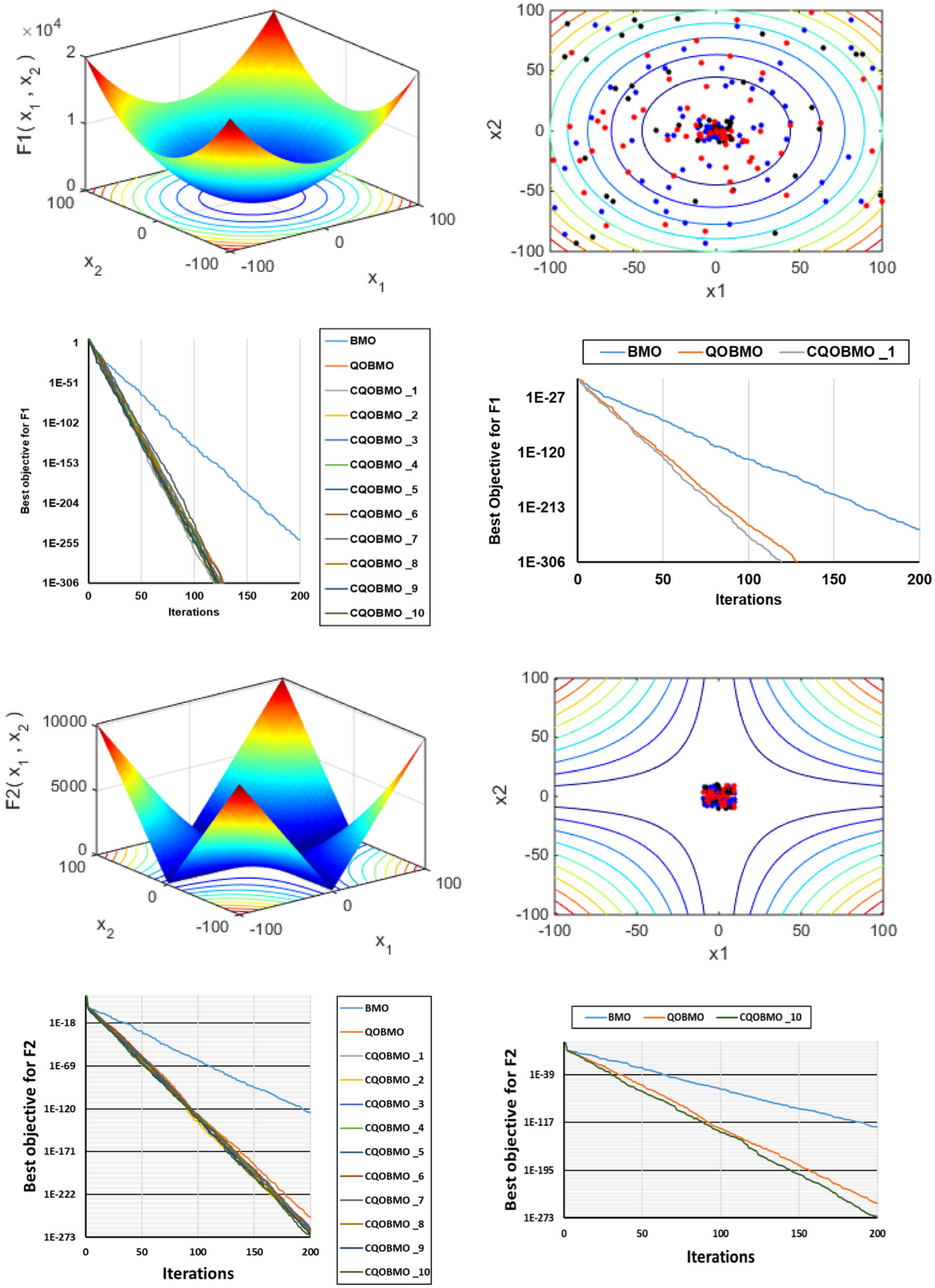

FIGURE 8 Performance characteristics of the optimization algorithms.

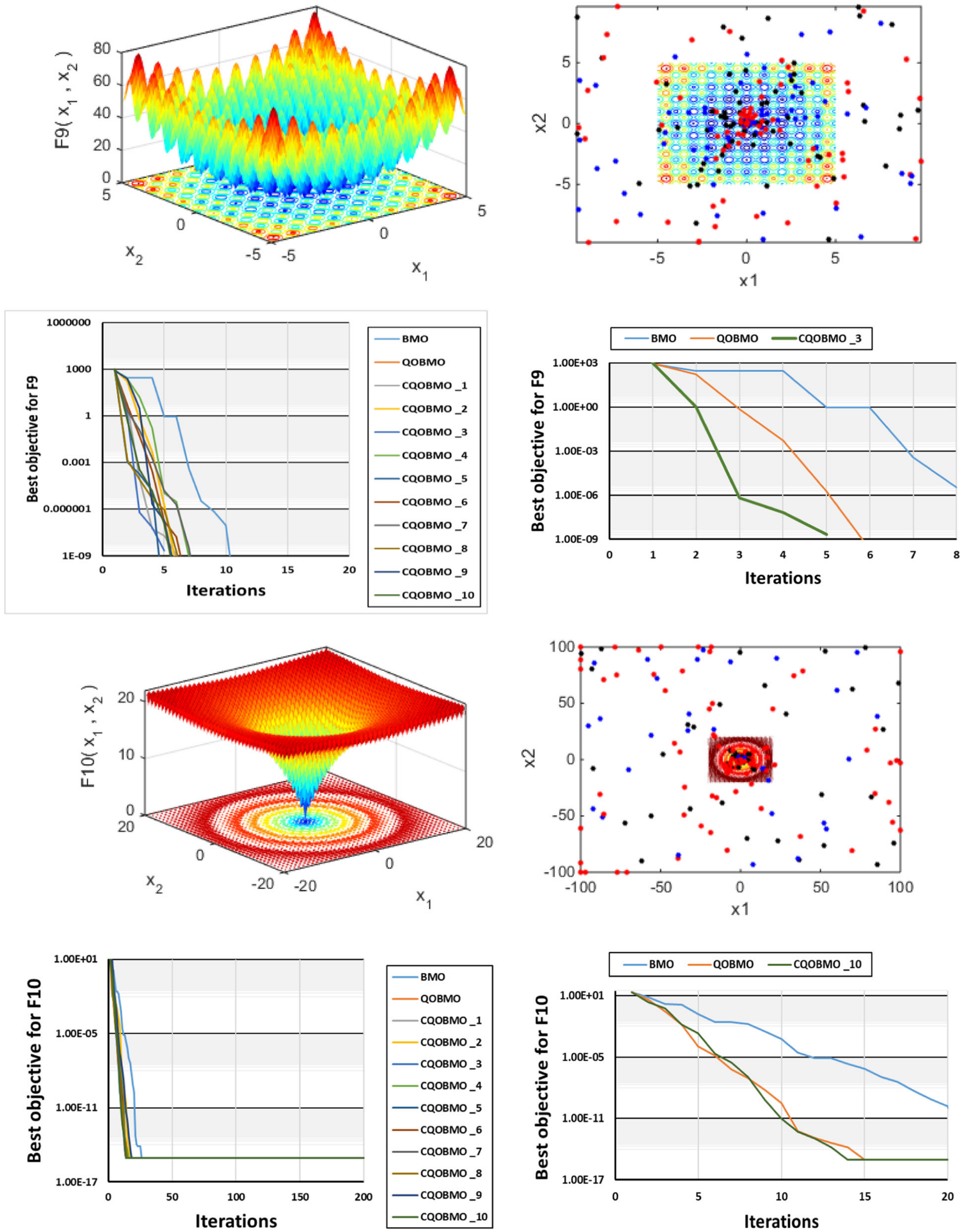

FIGURE 8 Continued

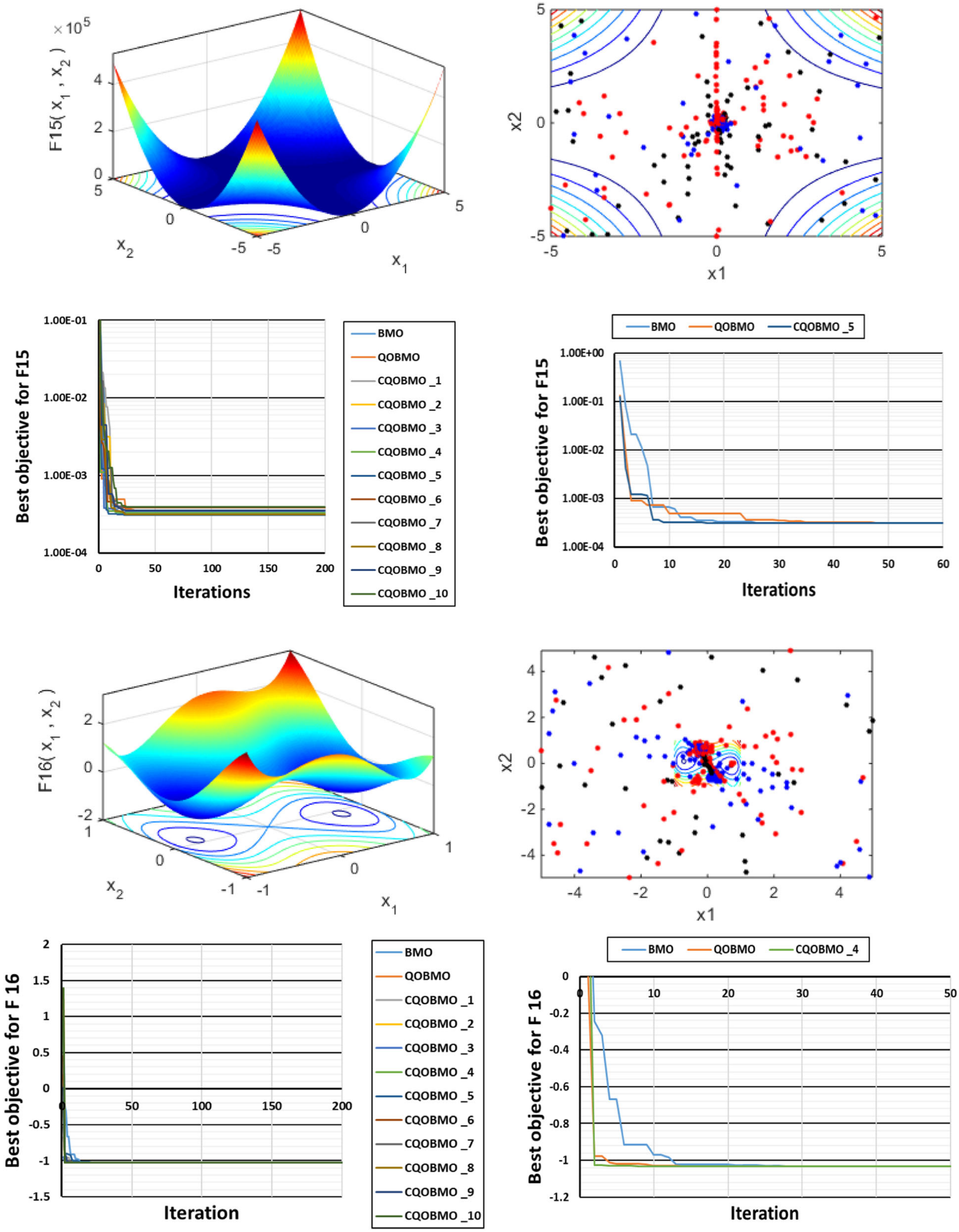

FIGURE 8 Continued

TABLE 4 Statistical analysis for the second group of the benchmarks (F8–F14) using Choatic maps.

		BMO	CBMO _1	CBMO _2	CBMO _3	CBMO _4	CBMO _5	CBMO _6	CBMO _7	CBMO _8	CBMO _9	CBMO _10
F8	Best	−1.71E+03	−6.83E+02	−6.88E+02	−6.90E+02	−6.91E+02	−5.94E+02	−6.48E+02	−6.42E+02	−7.19E+02	−9.08E+02	−7.31E+02
	Avg	**−1.53E+03**	−4.95E+02	−5.00E+02	−4.71E+02	−5.26E+02	−4.83E+02	−4.95E+02	−4.83E+02	−4.87E+02	−5.11E+02	−4.91E+02
	worst	**−9.95E+02**	−3.30E+02	−3.00E+02	−3.48E+02	−4.00E+02	−3.88E+02	−3.38E+02	−3.43E+02	−3.16E+02	−3.39E+02	−3.14E+02
F9	Best	**0.00E+00**	**0.00E+00**	**0.00E+00**	**0.00E+00**	**0.00E+00**	**0.00E+00**	**0.00E+00**	**0.00E+00**	**0.00E+00**	**0.00E+00**	**0.00E+00**
	Avg	**0.00E+00**	**0.00E+00**	**0.00E+00**	**0.00E+00**	**0.00E+00**	**0.00E+00**	**0.00E+00**	**0.00E+00**	**0.00E+00**	**0.00E+00**	**0.00E+00**
	worst	**0.00E+00**	**0.00E+00**	**0.00E+00**	**0.00E+00**	**0.00E+00**	**0.00E+00**	**0.00E+00**	**0.00E+00**	**0.00E+00**	**0.00E+00**	**0.00E+00**
F10	Best	**8.88E-16**	**8.88E-16**	**8.88E-16**	**8.88E-16**	**8.88E-16**	**8.88E-16**	**8.88E-16**	**8.88E-16**	**8.88E-16**	**8.88E-16**	**8.88E-16**
	Avg	**8.88E-16**	**8.88E-16**	**8.88E-16**	**8.88E-16**	**8.88E-16**	**8.88E-16**	**8.88E-16**	**8.88E-16**	**8.88E-16**	**8.88E-16**	**8.88E-16**
	worst	**8.88E-16**	**8.88E-16**	**8.88E-16**	**8.88E-16**	**8.88E-16**	**8.88E-16**	**8.88E-16**	**8.88E-16**	**8.88E-16**	**8.88E-16**	**8.88E-16**
F11	Best	**0.00E+00**	**0.00E+00**	**0.00E+00**	**0.00E+00**	**0.00E+00**	**0.00E+00**	**0.00E+00**	**0.00E+00**	**0.00E+00**	**0.00E+00**	**0.00E+00**
	Avg	**0.00E+00**	**0.00E+00**	**0.00E+00**	**0.00E+00**	**0.00E+00**	**0.00E+00**	**0.00E+00**	**0.00E+00**	**0.00E+00**	**0.00E+00**	**0.00E+00**
	worst	**0.00E+00**	**0.00E+00**	**0.00E+00**	**0.00E+00**	**0.00E+00**	**0.00E+00**	**0.00E+00**	**0.00E+00**	**0.00E+00**	**0.00E+00**	**0.00E+00**
F12	Best	3.20E-02	6.02E-01	3.26E-01	3.84E-01	5.95E-01	5.03E-01	6.64E-01	4.57E-01	5.09E-01	4.17E-01	3.36E-01
	Avg	**6.83E-02**	1.02E+00	9.71E-01	1.02E+00	1.08E+00	1.16E+00	1.07E+00	9.86E-01	1.02E+00	9.61E-01	1.03E+00
	worst	**1.20E-01**	1.60E+00	1.46E+00	1.43E+00	1.52E+00	1.56E+00	1.63E+00	1.57E+00	1.52E+00	1.53E+00	1.66E+00
F13	Best	**1.41E+00**	2.99E+00	2.99E+00	2.99E+00	2.99E+00	2.99E+00	2.99E+00	2.62E+00	2.65E+00	2.99E+00	2.99E+00
	Avg	**2.92E+00**	3.00E+00	3.00E+00	3.00E+00	3.00E+00	3.00E+00	3.00E+00	2.99E+00	2.99E+00	3.00E+00	3.00E+00
	worst	**2.98E+00**	3.00E+00	3.00E+00	3.00E+00	3.00E+00	3.00E+00	3.00E+00	3.00E+00	3.00E+00	3.00E+00	3.00E+00
F14	Best	1.99E+00	1.12E+00	1.91E+00	2.08E+00	1.29E+00	1.99E+00	**9.99E-01**	9.98E-01	1.99E+00	1.49E+00	1.00E+00
	Avg	9.71E+00	9.50E+00	9.52E+00	1.06E+01	9.50E+00	9.77E+00	8.77E+00	8.55E+00	9.42E+00	9.96E+00	**8.09E+00**
	worst	1.27E+01	1.27E+01	1.27E+01	1.27E+01	1.27E+01	1.27E+01	1.27E+01	1.27E+01	1.27E+01	1.27E+01	**1.27E+01**

TABLE 5 Statistical analysis for the second group of the benchmarks (F8–F14) using chaotic maps and quasi oppositional.

		BMO	QOBMO	CQOBMO _1	CQOBMO _2	CQOBMO _3	CQOBMO _4	CQOBMO _5	CQOBMO _6	CQOBMO _7	CQOBMO _8	CQOBMO _9	CQOBMO _10
F8	Best	−1.71E+03	**−1.70E+03**	−6.29E+02	−7.85E+02	−7.57E+02	−6.49E+02	−6.92E+02	−7.10E+02	−7.32E+02	−7.27E+02	−7.06E+02	−7.05E+02
	Avg	**−1.53E+03**	−1.44E+03	−4.86E+02	−5.24E+02	−5.02E+02	−4.93E+02	−5.15E+02	−5.36E+02	−4.96E+02	−4.99E+02	−5.32E+02	−5.20E+02
	worst	**−9.95E+02**	−9.87E+02	−3.23E+02	−3.82E+02	−3.50E+02	−3.82E+02	−3.52E+02	−3.64E+02	−3.49E+02	−3.34E+02	−3.38E+02	−3.94E+02
F9	Best	**0.00E+00**	**0.00E+00**	**0.00E+00**	**0.00E+00**	**0.00E+00**	**0.00E+00**	**0.00E+00**	**0.00E+00**	**0.00E+00**	**0.00E+00**	**0.00E+00**	**0.00E+00**
	Avg	**0.00E+00**	**0.00E+00**	**0.00E+00**	**0.00E+00**	**0.00E+00**	**0.00E+00**	**0.00E+00**	**0.00E+00**	**0.00E+00**	**0.00E+00**	**0.00E+00**	**0.00E+00**
	worst	**0.00E+00**	**0.00E+00**	**0.00E+00**	**0.00E+00**	**0.00E+00**	**0.00E+00**	**0.00E+00**	**0.00E+00**	**0.00E+00**	**0.00E+00**	**0.00E+00**	**0.00E+00**
F10	Best	**8.88E-16**	**8.88E-16**	**8.88E-16**	**8.88E-16**	**8.88E-16**	**8.88E-16**	**8.88E-16**	**8.88E-16**	**8.88E-16**	**8.88E-16**	**8.88E-16**	**8.88E-16**
	Avg	**8.88E-16**	**8.88E-16**	**8.88E-16**	**8.88E-16**	**8.88E-16**	**8.88E-16**	**8.88E-16**	**8.88E-16**	**8.88E-16**	**8.88E-16**	**8.88E-16**	**8.88E-16**
	worst	**8.88E-16**	**8.88E-16**	**8.88E-16**	**8.88E-16**	**8.88E-16**	**8.88E-16**	**8.88E-16**	**8.88E-16**	**8.88E-16**	**8.88E-16**	**8.88E-16**	**8.88E-16**
F11	Best	**0.00E+00**	**0.00E+00**	**0.00E+00**	**0.00E+00**	**0.00E+00**	**0.00E+00**	**0.00E+00**	**0.00E+00**	**0.00E+00**	**0.00E+00**	**0.00E+00**	**0.00E+00**
	Avg	**0.00E+00**	**0.00E+00**	**0.00E+00**	**0.00E+00**	**0.00E+00**	**0.00E+00**	**0.00E+00**	**0.00E+00**	**0.00E+00**	**0.00E+00**	**0.00E+00**	**0.00E+00**
	worst	**0.00E+00**	**0.00E+00**	**0.00E+00**	**0.00E+00**	**0.00E+00**	**0.00E+00**	**0.00E+00**	**0.00E+00**	**0.00E+00**	**0.00E+00**	**0.00E+00**	**0.00E+00**
F12	Best	3.20E-02	**2.68E-02**	3.29E-01	5.94E-01	5.69E-01	3.77E-01	5.71E-01	6.08E-01	4.64E-01	3.94E-01	5.61E-01	4.33E-01
	Avg	**6.83E-02**	6.94E-02	9.66E-01	9.04E-01	8.83E-01	9.34E-01	9.50E-01	9.01E-01	8.99E-01	8.70E-01	8.75E-01	8.35E-01
	worst	**1.20E-01**	2.99E-01	1.55E+00	1.34E+00	1.57E+00	1.47E+00	1.23E+00	1.47E+00	1.49E+00	1.50E+00	1.19E+00	1.20E+00
F13	Best	**1.41E+00**	2.97E+00	2.64E+00	2.77E+00	2.94E+00	2.37E+00	2.99E+00	2.99E+00	2.85E+00	2.99E+00	2.87E+00	2.99E+00
	Avg	**2.92E+00**	2.97E+00	2.99E+00	2.99E+00	2.99E+00	2.98E+00	3.00E+00	3.00E+00	2.99E+00	3.00E+00	2.99E+00	3.00E+00
	worst	**2.98E+00**	2.98E+00	3.00E+00	3.00E+00	3.00E+00	3.00E+00	3.00E+00	3.00E+00	3.00E+00	3.00E+00	3.00E+00	3.00E+00
F14	Best	1.99E+00	**9.98E-01**	1.01E+00	3.59E+00	1.77E+00	9.99E-01	1.22E+00	1.28E+00	1.99E+00	1.68E+00	1.25E+00	**9.99E-01**
	Avg	9.71E+00	8.55E+00	8.13E+00	9.16E+00	9.68E+00	**7.49E+00**	9.11E+00	7.75E+00	7.50E+00	8.29E+00	8.98E+00	7.76E+00
	worst	1.27E+01	1.27E+01	1.27E+01	1.27E+01	1.27E+01	**1.27E+01**	1.27E+01	1.27E+01	1.27E+01	1.27E+01	1.27E+01	1.27E+01

TABLE 6 Statistical analysis for the third group of the benchmarks (F15-F23) using chaotic maps.

		BMO	CBMO _1	CBMO _2	CBMO _3	CBMO _4	CBMO _5	CBMO _6	CBMO _7	CBMO _8	CBMO _9	CBMO _10
F15	Best	**3.08E-04**	3.40E-04	6.17E-04	3.77E-04	3.22E-04	3.67E-04	3.68E-04	3.92E-04	**3.08E-04**	3.12E-04	3.18E-04
	Avg	4.56E-04	6.40E-03	6.30E-03	8.61E-03	7.42E-03	1.36E-02	9.64E-03	1.14E-02	7.04E-03	9.32E-03	9.84E-03
	worst	1.33E-03	3.13E-02	2.72E-02	3.74E-02	2.87E-02	6.84E-02	6.68E-02	7.21E-02	3.27E-02	6.40E-02	6.44E-02
F16	Best	**−1.03E+00**	**−1.03E+00**	**−1.03E+00**	**−1.03E+00**	**−1.03E+00**	**−1.03E+00**	**−1.03E+00**	**−1.03E+00**	**−1.03E+00**	**−1.03E+00**	**−1.03E+00**
	Avg	**−1.03E+00**	−9.19E-01	−9.13E-01	−9.87E-01	−9.50E-01	−9.12E-01	−9.46E-01	−9.40E-01	−9.24E-01	−9.26E-01	−9.79E-01
	worst	**−1.02E+00**	−3.45E-01	−2.47E-01	−7.89E-01	−3.77E-01	−3.09E-01	−5.39E-01	−7.40E-01	−4.74E-01	−5.96E-01	−7.06E-01
F17	Best	**3.98E-01**	**3.98E-01**	**3.98E-01**	**3.98E-01**	**3.98E-01**	**3.98E-01**	**3.98E-01**	**3.98E-01**	**3.98E-01**	**3.98E-01**	**3.98E-01**
	Avg	**3.98E-01**	6.88E-01	5.02E-01	4.42E-01	6.33E-01	4.77E-01	5.11E-01	6.26E-01	5.82E-01	5.14E-01	4.56E-01
	worst	**3.98E-01**	6.08E+00	1.67E+00	7.76E-01	6.19E+00	1.05E+00	1.87E+00	2.21E+00	3.21E+00	2.38E+00	1.00E+00
F18	Best	**3.00E+00**	**3.00E+00**	**3.00E+00**	**3.00E+00**	**3.00E+00**	**3.00E+00**	**3.00E+00**	**3.00E+00**	**3.00E+00**	**3.00E+00**	**3.00E+00**
	Avg	**3.00E+00**	1.53E+01	9.49E+00	8.18E+00	9.22E+00	1.11E+01	1.22E+01	9.14E+00	7.50E+00	1.01E+01	9.31E+00
	worst	**3.00E+00**	6.52E+01	3.13E+01	3.69E+01	3.40E+01	3.18E+01	5.45E+01	3.71E+01	3.00E+01	3.49E+01	3.02E+01
F19	Best	**−3.00E-01**	**−3.00E-01**	**−3.00E-01**	**−3.00E-01**	**−3.00E-01**	**−3.00E-01**	**−3.00E-01**	**−3.00E-01**	**−3.00E-01**	**−3.00E-01**	**−3.00E-01**
	Avg	**−3.00E-01**	**−3.00E-01**	**−3.00E-01**	**−3.00E-01**	**−3.00E-01**	**−3.00E-01**	**−3.00E-01**	**−3.00E-01**	**−3.00E-01**	**−3.00E-01**	**−3.00E-01**
	worst	**−3.00E-01**	**−3.00E-01**	**−3.00E-01**	**−3.00E-01**	**−3.00E-01**	**−3.00E-01**	**−3.00E-01**	**−3.00E-01**	**−3.00E-01**	**−3.00E-01**	**−3.00E-01**
F20	Best	**−3.32E+00**	−2.93E+00	−3.06E+00	−2.80E+00	−2.97E+00	−2.74E+00	−3.04E+00	−2.99E+00	−3.28E+00	−2.89E+00	−2.61E+00
	Avg	−3.28E+00	−1.90E+00	−1.99E+00	−1.87E+00	−1.82E+00	−1.78E+00	−1.82E+00	−1.76E+00	−1.99E+00	−1.95E+00	−1.66E+00
	worst	−3.02E+00	−9.47E-01	−1.27E+00	−9.85E-01	−8.43E-01	−8.70E-01	−5.18E-01	−4.92E-01	−7.32E-01	−8.82E-01	−7.73E-01
F21	Best	−5.06E+00	−5.03E+00	−7.64E+00	−7.07E+00	−6.43E+00	−8.09E+00	**−9.86E+00**	−5.86E+00	−6.24E+00	−7.56E+00	−5.90E+00
	Avg	−5.06E+00	−4.41E+00	−4.58E+00	−4.68E+00	−4.94E+00	−4.68E+00	−4.85E+00	−4.57E+00	−4.68E+00	−4.79E+00	−4.78E+00
	worst	−5.06E+00	−2.70E+00	−3.17E+00	−2.61E+00	−4.13E+00	−2.86E+00	−2.96E+00	−3.01E+00	−2.96E+00	−3.55E+00	−4.16E+00
F22	Best	−5.09E+00	**−1.03E+01**	−5.94E+00	−5.68E+00	−8.33E+00	−5.09E+00	−6.78E+00	−6.06E+00	−9.17E+00	−7.57E+00	−8.86E+00
	Avg	−5.09E+00	−5.02E+00	−4.61E+00	−4.65E+00	**−5.14E+00**	−4.60E+00	−4.73E+00	−4.77E+00	−4.80E+00	−4.81E+00	−4.78E+00
	worst	−5.09E+00	−3.71E+00	−3.65E+00	−3.02E+00	−3.64E+00	−3.19E+00	−3.81E+00	−2.80E+00	−3.40E+00	−3.37E+00	−2.27E+00
F23	Best	−5.13E+00	**−1.03E+01**	−7.20E+00	−5.64E+00	−6.52E+00	−7.93E+00	−7.07E+00	−5.10E+00	−9.46E+00	−6.21E+00	−5.93E+00
	Avg	−5.13E+00	−4.94E+00	−4.73E+00	−4.73E+00	−4.97E+00	−4.76E+00	−4.87E+00	−4.62E+00	−4.99E+00	−4.87E+00	−4.75E+00
	worst	−5.13E+00	−3.76E+00	−2.74E+00	−3.54E+00	−3.61E+00	−3.11E+00	−3.94E+00	−3.54E+00	−3.78E+00	−3.46E+00	−3.96E+00

TABLE 7 Statistical analysis for the third group of the benchmarks (F15-F23) using chaotic maps and quasi oppositional.

		BMO	QOBMO	CQOBMO _1	CQOBMO _2	CQOBMO _3	CQOBMO _4	CQOBMO _5	CQOBMO _6	CQOBMO _7	CQOBMO _8	CQOBMO _9	CQOBMO _10
F15	Best	**3.08E-04**	**3.08E-04**	3.18E-04	**3.12E-04**	3.36E-04	3.29E-04	**3.10E-04**	3.84E-04	**3.13E-04**	**3.14E-04**	3.53E-04	3.95E-04
	Avg	4.56E-04	**4.46E-04**	5.35E-03	2.76E-03	2.96E-03	4.12E-03	3.82E-03	4.48E-03	5.00E-03	1.02E-02	6.87E-03	3.95E-03
	worst	1.33E-03	**7.62E-04**	7.44E-02	1.19E-02	1.11E-02	3.42E-02	1.58E-02	2.68E-02	2.21E-02	5.37E-02	3.73E-02	1.32E-02
F16	Best	**−1.03E+00**	**−1.03E+00**	**−1.03E+00**	**−1.03E+00**	**−1.03E+00**	**−1.03E+00**	**−1.03E+00**	**−1.03E+00**	**−1.03E+00**	**−1.03E+00**	**−1.03E+00**	**−1.03E+00**
	Avg	**−1.03E+00**	**−1.03E+00**	−9.38E-01	−9.78E-01	−9.73E-01	−1.01E+00	−9.48E-01	−9.69E-01	−9.78E-01	−9.70E-01	−9.39E-01	−9.73E-01
	worst	**−1.02E+00**	**−1.03E+00**	−6.24E-03	−4.74E-01	−3.97E-01	−8.75E-01	−4.99E-01	−6.48E-01	−4.36E-01	−5.39E-01	−1.95E-01	−5.80E-01
F17	Best	**3.98E-01**	**3.98E-01**	**3.98E-01**	**3.98E-01**	**3.98E-01**	**3.98E-01**	**3.98E-01**	**3.98E-01**	**3.98E-01**	**3.98E-01**	**3.98E-01**	**3.98E-01**
	Avg	**3.98E-01**	**3.98E-01**	4.71E-01	4.26E-01	5.30E-01	4.76E-01	4.56E-01	6.16E-01	4.62E-01	4.44E-01	4.48E-01	4.49E-01
	worst	**3.98E-01**	**3.98E-01**	1.41E+00	7.75E-01	3.64E+00	1.23E+00	6.90E-01	2.22E+00	2.03E+00	1.23E+00	1.08E+00	1.38E+00
F18	Best	**3.00E+00**	**3.00E+00**	**3.00E+00**	**3.00E+00**	**3.00E+00**	**3.00E+00**	**3.00E+00**	**3.00E+00**	**3.00E+00**	**3.00E+00**	**3.00E+00**	**3.00E+00**
	Avg	**3.00E+00**	**3.00E+00**	7.47E+00	8.97E+00	7.50E+00	5.89E+00	7.55E+00	9.06E+00	1.02E+01	8.18E+00	8.02E+00	8.88E+00
	worst	**3.00E+00**	**3.00E+00**	3.00E+01	3.30E+01	3.00E+01	2.55E+01	3.48E+01	3.14E+01	3.10E+01	3.46E+01	3.21E+01	3.01E+01
F19	Best	**−3.00E-01**	**−3.00E-01**	**−3.00E-01**	**−3.00E-01**	**−3.00E-01**	**−3.00E-01**	**−3.00E-01**	**−3.00E-01**	**−3.00E-01**	**−3.00E-01**	**−3.00E-01**	**−3.00E-01**
	Avg	**−3.00E-01**	**−3.00E-01**	**−3.00E-01**	**−3.00E-01**	**−3.00E-01**	**−3.00E-01**	**−3.00E-01**	**−3.00E-01**	**−3.00E-01**	**−3.00E-01**	**−3.00E-01**	**−3.00E-01**
	worst	**−3.00E-01**	**−3.00E-01**	**−3.00E-01**	**−3.00E-01**	**−3.00E-01**	**−3.00E-01**	**−3.00E-01**	**−3.00E-01**	**−3.00E-01**	**−3.00E-01**	**−3.00E-01**	**−3.00E-01**
F20	Best	**−3.32E+00**	**−3.32E+00**	−2.78E+00	−3.01E+00	−2.86E+00	−2.73E+00	−3.11E+00	−3.15E+00	−3.18E+00	−3.10E+00	−3.22E+00	−2.85E+00
	Avg	−3.28E+00	**−3.30E+00**	−1.95E+00	−1.87E+00	−1.93E+00	−1.95E+00	−2.03E+00	−1.98E+00	−1.85E+00	−2.03E+00	−2.11E+00	−1.82E+00
	worst	−3.02E+00	**−3.13E+00**	−6.67E-01	−1.20E+00	−8.51E-01	−8.85E-01	−9.05E-01	−8.25E-01	−9.05E-01	−7.53E-01	−6.31E-01	−6.51E-01
F21	Best	−5.06E+00	**−1.02E+01**	**−1.02E+01**	**−1.02E+01**	−1.02E+01	−1.02E+01	−1.02E+01	**−1.02E+01**	−1.02E+01	−1.02E+01	−1.02E+01	−1.02E+01
	Avg	−5.06E+00	**−1.02E+01**	−1.01E+01	−1.01E+01	−1.01E+01	−1.01E+01	−1.01E+01	−1.01E+01	−1.01E+01	−1.01E+01	−1.00E+01	−1.01E+01
	worst	−5.06E+00	**−1.02E+01**	−9.79E+00	−9.79E+00	−9.54E+00	−9.97E+00	−9.76E+00	−9.39E+00	−9.83E+00	−9.74E+00	−9.13E+00	−1.00E+01
F22	Best	−5.09E+00	**−1.04E+01**	−1.04E+01	−1.04E+01	**−1.04E+01**	**−1.04E+01**	**−1.04E+01**	**−1.04E+01**	−1.04E+01	−1.04E+01	−1.04E+01	**−1.04E+01**
	Avg	−5.09E+00	**−1.04E+01**	−1.03E+01	−1.04E+01	−1.03E+01	−1.04E+01	−1.04E+01	−1.04E+01	−1.03E+01	−1.04E+01	−1.04E+01	−1.03E+01
	worst	−5.09E+00	**−1.04E+01**	−9.90E+00	−1.02E+01	−1.01E+01	−1.01E+01	−1.01E+01	−9.88E+00	−1.01E+01	−1.02E+01	−1.01E+01	−8.90E+00
F23	Best	−5.13E+00	**−1.05E+01**	−1.05E+01	−1.05E+01	−1.05E+01	−1.05E+01	−1.05E+01	−1.05E+01	**−1.05E+01**	−1.05E+01	−1.05E+01	−1.05E+01
	Avg	−5.13E+00	**−1.05E+01**	−1.05E+01	−1.05E+01	−1.05E+01	−1.05E+01	−1.05E+01	−1.05E+01	−1.05E+01	−1.05E+01	−1.05E+01	−1.05E+01
	worst	−5.13E+00	**−1.05E+01**	−9.93E+00	−9.44E+00	−1.01E+01	−9.94E+00	−1.02E+01	−9.64E+00	−1.03E+01	−1.02E+01	−1.01E+01	−1.04E+01

TABLE 8 Results of the Wilcoxon signed-rank test BMO and the other algorithms for the first group of the benchmarks (F1–F7).

		QOBMO	CQOBMO _1	CQOBMO _2	CQOBMO _3	CQOBMO _4	CQOBMO _5	CQOBMO _6	CQOBMO _7	CQOBMO _8	CQOBMO _9	CQOBMO _10
F1	$\sum R^+$	0	0	0	0	0	0	0	0	0	0	0
	$\sum R^-$	−465	−465	−465	−465	−465	−465	−465	−465	−465	−465	−465
	p-value	1.78E-06	1.78E-06	1.78E-06	1.78E-06	1.78E-06	1.78E-06	1.78E-06	1.78E-06	1.78E-06	1.78E-06	1.78E-06
F2	$\sum R^+$	0	0	0	0	0	0	0	0	0	0	0
	$\sum R^-$	−465	−465	−465	−465	−465	−465	−465	−465	−465	−465	−465
	p-value	1.78E-06	1.78E-06	1.78E-06	1.78E-06	1.78E-06	1.78E-06	1.78E-06	1.78E-06	1.78E-06	1.78E-06	1.78E-06
F3	$\sum R^+$	0	0	0	0	0	0	0	0	0	0	0
	$\sum R^-$	−465	−465	−465	−465	−465	−465	−465	−465	−465	−465	−465
	p-value	1.78E-06	1.78E-06	1.78E-06	1.78E-06	1.78E-06	1.78E-06	1.78E-06	1.78E-06	1.78E-06	1.78E-06	1.78E-06
F4	$\sum R^+$	0	0	0	0	0	0	0	0	0	0	0
	$\sum R^-$	−465	−465	−465	−465	−465	−465	−465	−465	−465	−465	−465
	p-value	1.78E-06	1.78E-06	1.78E-06	1.78E-06	1.78E-06	1.78E-06	1.78E-06	1.78E-06	1.78E-06	1.78E-06	1.78E-06
F5	$\sum R^+$	157	465	465	465	465	465	465	465	465	465	465
	$\sum R^-$	−308	0	0	0	0	0	0	0	0	0	0
	p-value	1.22E-01	1.78E-06	1.78E-06	1.78E-06	1.78E-06	1.78E-06	1.78E-06	1.78E-06	1.78E-06	1.78E-06	1.78E-06
F6	$\sum R^+$	102	465	465	465	465	465	465	465	465	465	465
	$\sum R^-$	−363	0	0	0	0	0	0	0	0	0	0
	p-value	7.38E-03	1.78E-06	1.78E-06	1.78E-06	1.78E-06	1.78E-06	1.78E-06	1.78E-06	1.78E-06	1.78E-06	1.78E-06
F7	$\sum R^+$	98	99	136	166	108	102	152	100	101	117	99
	$\sum R^-$	−367	−366	−329	−299	−357	−363	−313	−365	−364	−348	−366
	p-value	5.76E-03	6.13E-03	4.77E-02	1.73E-01	1.06E-02	7.38E-03	9.88E-02	6.52E-03	6.94E-03	1.78E-02	6.13E-03

TABLE 9 Results of the Wilcoxon signed-rank test BMO and the other algorithms for the second group of the benchmarks (F8–F14).

		QOBMO	CQOBMO _1	CQOBMO _2	CQOBMO _3	CQOBMO _4	CQOBMO _5	CQOBMO _6	CQOBMO _7	CQOBMO _8	CQOBMO _9	CQOBMO _10
F8	$\sum R^+$	325	465	465	465	465	465	465	465	465	465	465
	$\sum R^-$	−140	0	0	0	0	0	0	0	0	0	0
	p-value	5.78E-02	1.78E-06	1.78E-06	1.78E-06	1.78E-06	1.78E-06	1.78E-06	1.78E-06	1.78E-06	1.78E-06	1.78E-06
F9	$\sum R^+$	There are not variations. Wilcoxon test can't be performed										
	$\sum R^-$											
	p-value											
F10	$\sum R^+$	There are not variations. Wilcoxon test can't be performed										
	$\sum R^-$											
	p-value											
F11	$\sum R^+$	There are not variations. Wilcoxon test can't be performed										
	$\sum R^-$											
	p-value											
F12	$\sum R^+$	171	465	465	465	465	465	465	465	465	465	465
	$\sum R^-$	−294	0	0	0	0	0	0	0	0	0	0
	p-value	2.08E-01	1.78E-06	1.78E-06	1.78E-06	1.78E-06	1.78E-06	1.78E-06	1.78E-06	1.78E-06	1.78E-06	1.78E-06
F13	$\sum R^+$	270	436	436	436	436	465	465	436	465	436	465
	$\sum R^-$	−195	−29	−29	−29	−29	0	0	−29	0	−29	0
	p-value	4.44E-01	2.91E-05	2.91E-05	2.91E-05	2.91E-05	1.78E-06	1.78E-06	2.91E-05	1.78E-06	2.91E-05	1.78E-06
F14	$\sum R^+$	215	250	315	181	281	207	184	221	247	197	296
	$\sum R^-$	−250	−215	−150	−284	−184	−258	−281	−244	−218	−268	−167
	p-value	7.23E-01	7.23E-01	9.07E-02	2.92E-01	3.21E-01	6.04E-01	3.21E-01	8.17E-01	7.69E-01	4.68E-01	1.86E-01

TABLE 10 Results of the Wilcoxon signed-rank test BMO and the other algorithms for the third group of the benchmarks (F15–F23).

		QOBMO	CQOBMO _1	CQOBMO _2	CQOBMO _3	CQOBMO _4	CQOBMO _5	CQOBMO _6	CQOBMO _7	CQOBMO _8	CQOBMO _9	CQOBMO _10
F15	$\sum R^+$	255	456	460	443	449	439	464	458	455	460	465
	$\sum R^-$	−210	−9	−5	−22	−16	−26	−1	−7	−10	−5	0
	p-value	6.47E-01	4.39E-06	2.95E-06	1.53E-05	8.67E-06	2.21E-05	1.97E-06	3.60E-06	4.85E-06	2.95E-06	1.78E-06
F16	$\sum R^+$	No change	457	442	465	465	448	465	448	446	449	452
	$\sum R^-$		−8	−23	0	0	−17	0	−17	−19	−16	−13
	p-value		3.98E-06	1.68E-05	1.78E-06	1.78E-06	9.54E-06	1.78E-06	9.54E-06	1.15E-05	8.67E-06	6.49E-06
F17	$\sum R^+$	No change	465	465	465	464	465	464	465	465	464	465
	$\sum R^-$		0	0	0	−1	0	−1	0	0	−1	0
	p-value		1.78E-06	1.78E-06	1.78E-06	1.97E-06	1.78E-06	1.97E-06	1.78E-06	1.78E-06	1.97E-06	1.78E-06
F18	$\sum R^+$	No change	465	464	465	465	465	465	465	465	465	465
	$\sum R^-$		0	−1	0	0	0	0	0	0	0	0
	p-value		1.78E-06	1.97E-06	1.78E-06	1.78E-06	1.78E-06	1.78E-06	1.78E-06	1.78E-06	1.78E-06	1.78E-06
F19	$\sum R^+$	There are not variations . Wilcoxon test can′t be performed										
	$\sum R^-$											
	p-value											
F20	$\sum R^+$	268	465	465	465	465	465	465	465	465	465	465
	$\sum R^-$	−197	0	0	0	0	0	0	0	0	0	0
	p-value	4.68E-01	1.78E-06	1.78E-06	1.78E-06	1.78E-06	1.78E-06	1.78E-06	1.78E-06	1.78E-06	1.78E-06	1.78E-06
F21	$\sum R^+$	0	0	0	0	0	0	0	0	0	0	0
	$\sum R^-$	−465	−465	−465	−465	−465	−465	−465	−465	−465	−465	−465
	p-value	1.78E-06	1.78E-06	1.78E-06	1.78E-06	1.78E-06	1.78E-06	1.78E-06	1.78E-06	1.78E-06	1.78E-06	1.78E-06
F22	$\sum R^+$	0	0	0	0	0	0	0	0	0	0	0
	$\sum R^-$	−465	−465	−465	−465	−465	−465	−465	−465	−465	−465	−465
	p-value	1.78E-06	1.78E-06	1.78E-06	1.78E-06	1.78E-06	1.78E-06	1.78E-06	1.78E-06	1.78E-06	1.78E-06	1.78E-06
F23	$\sum R^+$	0	0	0	0	0	0	0	0	0	0	0
	$\sum R^-$	−465	−465	−465	−465	−465	−465	−465	−465	−465	−465	−465
	p-value	1.78E-06	1.78E-06	1.78E-06	1.78E-06	1.78E-06	1.78E-06	1.78E-06	1.78E-06	1.78E-06	1.78E-06	1.78E-06

TABLE 11 The average computation time of all simulations per (sec).

Benchmark	BMO	QOBMO	CBMO_7	CQOBMO_7	Benchmark	BMO	QOBMO	CBMO_7	CQOBMO_7
F1	0.215	0.419	0.169	0.356	F13	0.644	1.297	0.626	1.274
F2	0.195	0.394	0.172	0.364	F14	1.076	2.133	1.076	2.144
F3	0.524	1.078	0.526	1.064	F15	0.190	0.342	0.175	0.338
F4	0.190	0.369	0.169	0.356	F16	0.167	0.316	0.167	0.368
F5	0.227	0.444	0.207	0.430	F17	0.152	0.296	0.162	0.282
F6	0.193	0.384	0.170	0.350	F18	0.150	0.288	0.157	0.289
F7	0.343	0.702	0.328	0.648	F19	0.241	0.474	0.236	0.452
F8	0.233	0.451	0.213	0.452	F20	0.207	0.390	0.193	0.364
F9	0.193	0.381	0.175	0.366	F21	0.222	0.420	0.209	0.413
F10	0.200	0.415	0.184	0.393	F22	0.254	0.449	0.231	0.458
F11	0.231	0.449	0.219	0.435	F23	0.268	0.512	0.261	0.510
F12	0.671	1.364	0.640	1.317					

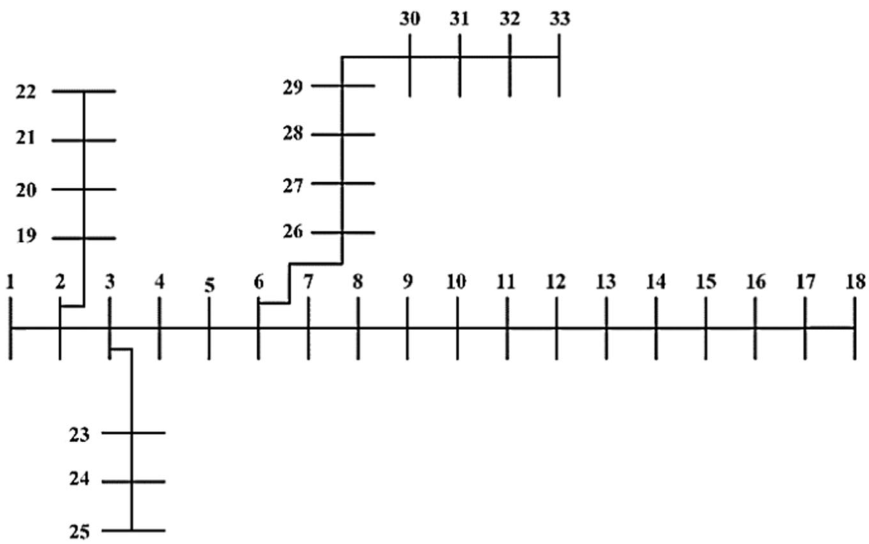

FIGURE 9 Illustration of the IEEE 33-bus connection lines.

solution to different optimization problems compared to the conventional BMO.

(4) Wilcoxon signed-rank test
To demonstrate the efficiency of the improved BMO methods based on the quasi opposition and the chaotic theories over the conventional BMO, a nonparametric statistical test is performed using Wilcoxon signed-rank test (WSRT).[81] When using WSRT, the R+ and R– related to the comparisons between two algorithms can be calculated and their p values can be obtained. $\sum R^{+}$ denotes the total of positive differences ranks for the problem in which the first algorithm outperformed the second, and $\sum R^{-}$ denotes the sum of ranks for the problem in which the second method exceeded the first.

In this study, there are 11 improved versions of the BMO; hence, the conventional BMO is used as a reference in the WSRT to demonstrate the efficiency of the improved methods. By using the BMO as a reference, the high value of $\sum R^{-}$ means that the improved method is better than the conventional BMO. The obtained results are summarized in Tables 8, 9, and 10 for the benchmarks' first, second, and third groups, respectively.

According to the obtained results, the overall number of $\sum R^{-}$ rankings w,v is higher than the total number of $\sum R^{+}$ difference rankings. However, WSRT cannot be used in the cases of F9, F10, F11, and F19 since there are no variances in the results. In addition, the p-value is computed. Consequently, this study proves that the

TABLE 12 Results of different optimization algorithms for DG allocation in IEEE 33-bus system.

Method	DG allocation		Power loss (kW)	LR %
	Location	Size (kW)		
CQOBMO_7	13	788.58	**73.29**	**65.26**
	24	889.58		
	30	1077.13		
QOBMO	14	874.6	73.5	65.16
	24	960.36		
	30	1012.29		
CBMO_7	13	658.43	73.87	64.82
	24	1065.61		
	30	1075.59		
BMO	14	749.59	75.81	64.04
	24	1234.59		
	30	771.50		
QOTLBO[83]	12	880.8	74.10	64.88
	24	1059.2		
	29	1071.4		
TLBO[83]	10	824.6	75.54	64.20
	24	1031.1		
	31	886.2		
BSOA[75]	13	632	89.05	57.76
	28	486		
	31	550		
LSF[69]	18	720	85.07	59.72
	33	810		
	25	900		
BFOA[76]	14	779	73.53	65.14
	25	880		
	30	1083		
Fuzzy -IAS[74]	32	2071	117.36	42.45
	30	1113.8		
	31	150.3		

improved versions of the BMO using the quasi opposition and chaos theories are able to find the optimal solution to different optimization problems.

(5) Time complexity analysis

To demonstrate the efficiency of the improved versions of the BMO algorithm, the average computation time for the 30 runs of all simulations is calculated and summarized in Table 11. The results

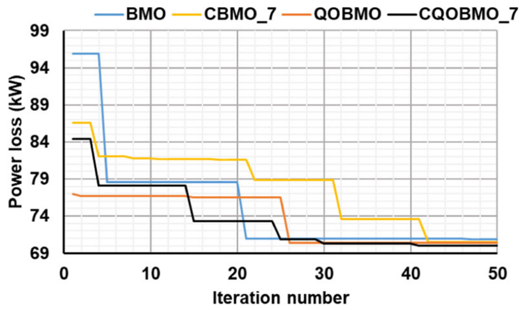

FIGURE 10 Convergence characteristics of the BMO, CBMO, QOBMO, and CQOBMO for the IEEE 33-bus test system.

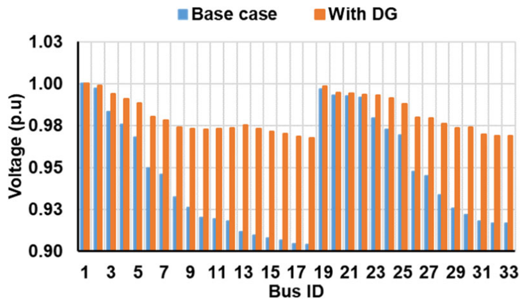

FIGURE 11 Enhancement of the IEEE 33-bus voltage profile using optimal DG allocation.

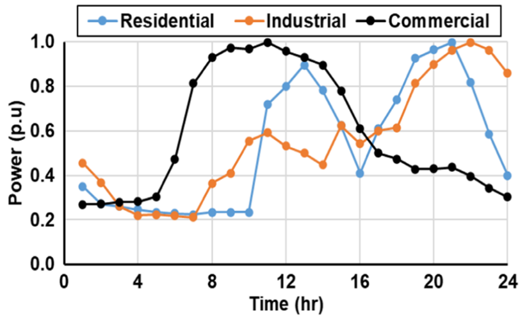

FIGURE 12 Residential, industrial, and commercial daily load curves.

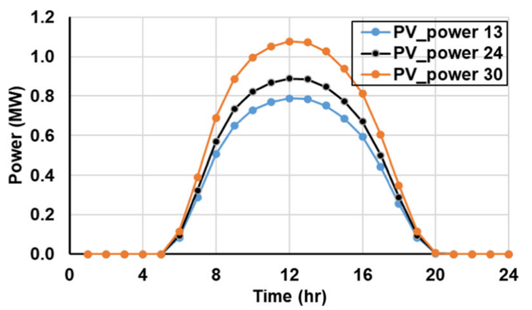

FIGURE 13 Photovoltaic output power at buses 13, 24, and 30.

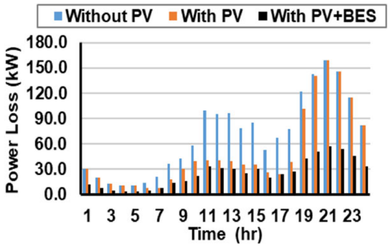

FIGURE 14 Power losses in IEEE 33-bus during 24 h at different case studies.

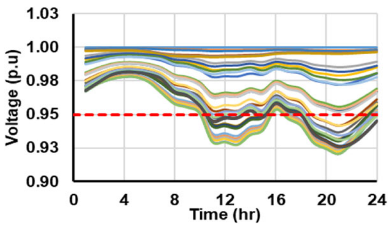

FIGURE 15 Voltage profile of IEEE 33-bus during 24 h at base case (without photovoltaic).

show that CBMO_7 takes the lowest time compared to all BMO versions. However, QOBMO takes more time due to the calculation of the quasi oppositional. the computation time in the CQOBMO_7 is decreased compared to the QOBMO which demonstrates the impact of the chaotic maps.

5.2 | DG allocation using the improved BMO

The problem of the DG allocation is studied using two IEEE test systems (IEEE 33-bus and IEEE 69-bus). The improved BMO based on the quasi oppositional and chaos map theories is applied to find the optimal size and location of the DG, then the PV power generation based on the uncertainty model with a daily load curve is applied to present the impact of the intermittent nature of the PV on the voltage profile and the power loss during 24 h. Finally, the improved method is employed to find the optimal PV+BES power, which minimizes the distribution system's total energy loss.

(1) IEEE 33-bus system

(a) Optimal size and location of DG using improved BMO

The improved methods are studied using the IEEE 33-bus test system.[82] The one-line diagram is given in Figure 9. The base case power flow results verified that the active power loss is 210.98 kW, where the reactive power losses are 143.14 kVAR. BMO, CBMO, QOBMO, and CQOBMO are applied to find the best solutions (sizes and locations) of the three DG units for reducing the power loss (objective function), and the results are given in Table 12.

It can be detected from Table 12 that using the CQOBMO_7, a loss reduction (LR) in the power loss quals 65.26% is achieved, which is higher than those obtained by LSF[69] (59.72%), Fuzzy-IAS[74] which is 42.45%, 57.76% given in BSOA,[75] 65.14% in BFOA,[76] TLBO[83] which reaches 64.20%, 64.88% in QOTLBO.[83]

Also, a comparison in the convergence characteristics between the improved methods and the conventional BMO is depicted in Figure 10. The figure efficiency of the CQOBMO_7 over the CBMO_7, QOBMO, and BMO. The impact of the DG placement on the voltage profile is displayed in Figure 11. It is evident that the optimal installation of the DGs in the distribution system leads to a significant enhancement in the voltage profile besides the minimization of power losses.

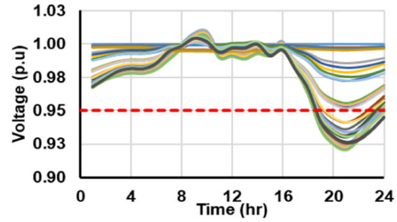

FIGURE 16 Voltage profile of IEEE 33-bus during 24 h with photovoltaic.

(b) The optimal size of PV + BES using improved BMO

The improved BMO based on the quasi oppositional and sine chaotic map is used in this section to find the optimal PV + BES size after approving its feasibility in the previous sections.

In this study, a combination of residential, industrial, and commercial daily load curves (see Figure 12) is adopted and used to present the variation in the load demand. However, the intermittent nature of the PV is modeled using uncertainty analysis. Hence, using the optimal sizes and location of the DG obtained earlier, time-series load flow is carried out using the daily load curves and PV power shown in Figure 13. The results show that the power loss increases at the base case (without PV) when high load demand is presented in Figure 14. In addition, the voltage

TABLE 13 The optimal size of PV + BES in IEEE 33-bus system.

Location	PV size (MW)	BES rated power (MW)	BES capacity (MW h)
Bus 13	1.28	0.79	5.97
Bus 24	1.74	1.11	9.16
Bus 30	1.66	0.99	8.54

Abbreviations: BES, battery energy storage; PV, photovoltaic.

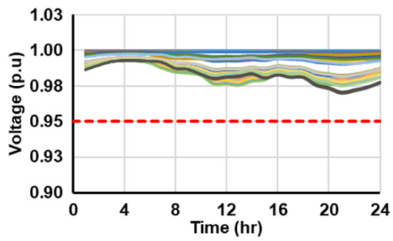

FIGURE 17 Voltage profile of IEEE 33-bus for 24 h with photovoltaic + battery energy storage.

profile of some buses is lower than the limits (0.95 p.u) as exhibited in Figure 15.
However, integrating PV at bus 13, 24, and 30 reduce the power loss and improve the voltage profile during the availability of the PV power, as displayed in Figures 14 and 16, respectively. However, the power loss is still high, and the voltage profile is still lower than the limits at the time when no PV power is injected (from 19:00 to 24:00).

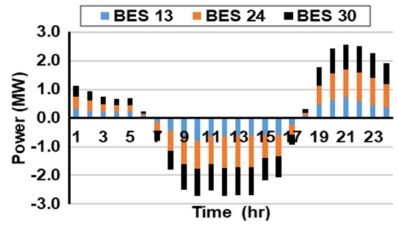

FIGURE 18 Charging/discharging powers of different battery energy storage integration in IEEE 33-bus.

TABLE 14 Daily energy losses for IEEE 33-bus.

Case	Energy losses (kW h)	Reduction %
Without PV	1673.94	-
With PV	1213.35	27.5
With PV + BES	602.35	64.0

Abbreviations: BES, battery energy storage; PV, photovoltaic.

BES is used with the PV to avoid this problem, and the optimal size of the PV + BES power during 24 h is calculated using the CQOBMO_7, then the final PV power is computed using (23). Hence, the optimal sizes of the PV and the BES are summarized in Table 13. Consequently, the integration of the PV + BES minimizes the power loss as presented in Figure 14 and enhances the voltage profile as shown in Figure 17.
Figure 18 shows the BES charging and discharging power at the optimal locations, and the BES

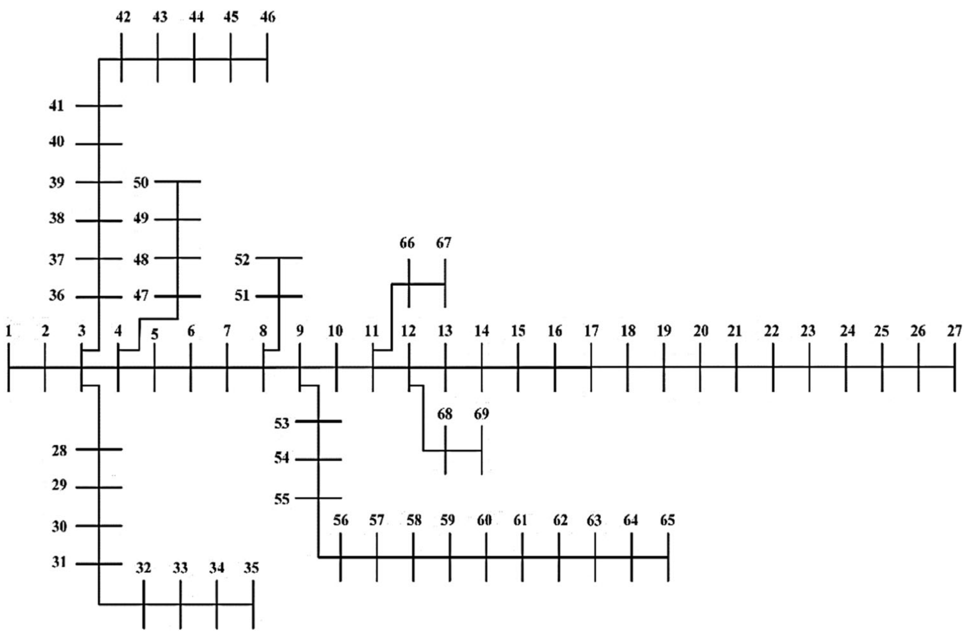

FIGURE 19 Illustration of the IEEE 69-bus connection lines.

TABLE 15 Results of different optimization algorithms for DG allocation in IEEE 69-bus system.

Method	DG allocation Location	Size (kW)	Power loss (kW)	LR %
CQOBMO_7	11	573.02	**70.05**	**68.86**
	18	355.20		
	61	1583.50		
QOBMO	21	246.45	70.43	68.69
	61	1704.45		
	66	489.5		
CBMO_7	10	371.74	70.44	68.69
	17	414.33		
	61	1833.01		
BMO	17	451.49	70.86	68.5
	55	569.4		
	61	1683.92		
QOTLBO[83]	18	533.4	71.63	68.17
	61	1198.6		
	63	567.2		
TLBO[83]	15	591.9	72.41	67.82
	61	818.8		
	63	900.3		
BFOA[76]	27	295.4	75.23	66.56
	65	446		
	61	1345.1		
GAPSO[77]	63	884.9	81.1	63.96
	61	1196		
	21	910.5		

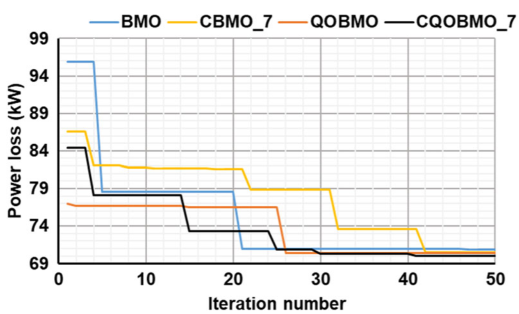

FIGURE 20 Convergence characteristics of the BMO, QOBMO, CBMO_7, and CQOBMO for IEEE 69-bus test system.

capacities are calculated based on the maximum charging power of each BES and given in Table 13. Table 14 proves the benefits of the PV + BES in reducing the total energy losses, where the reduction

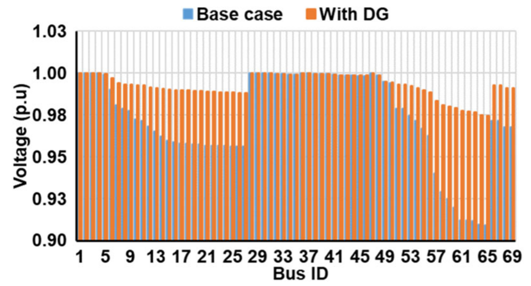

FIGURE 21 Enhancement of the IEEE 69-bus voltage profile using optimal DG allocation.

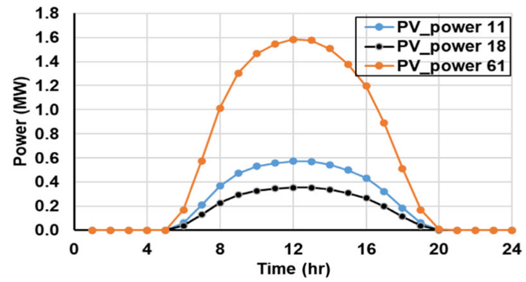

FIGURE 22 Photovoltaic output power at buses 11, 18, and 61.

reaches 64% compared to 27.5% in the case of using the PV.

(2) IEEE 69-Bus system
(a) Optimal size and location of DG using improved BMO

IEEE 69-bus is larger than the previous IEEE 33-bus, which is better to prove the performance of the improved methods. The full description of this system can be found in Baran and Wu,[84] and the connection line is revealed in Figure 19.

In the base case (without DG), The load flow calculation of the IEEE 69-bus system stated that 224.95 kW of the active power loss and 102.15 kVAR of the reactive power loss. Hence, three DG are suitably placed to minimize the power loss using the improved methods.

Table 15 yields the optimal allocations of the DGs in IEEE 69 bus using different optimization algorithms compared to the CQOBMO_7, the QOBMO, CBMO_7, and BMO. Evidence shows that the highest LR is 68.86%, which was obtained by CQOBMO_7 when integrated with three DG at 11, 18, and 61 with active powers equal to 573.02, 355.20, and 1583.50 kW, respectively. The convergence performance of CQOBMO_7, QOBMO, CBMO_7, and BMO is

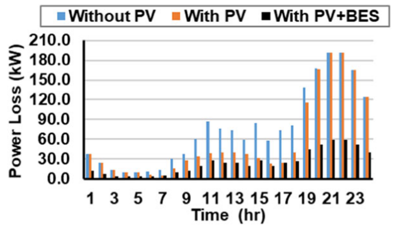

FIGURE 23 Power losses in IEEE 69-bus during 24 h at different case studies.

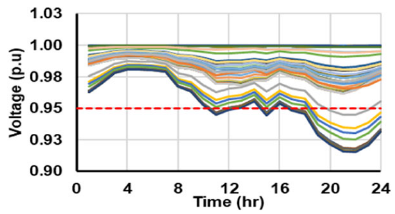

FIGURE 24 Voltage profile of IEEE 69 bus during 24 h at base case (without photovoltaic).

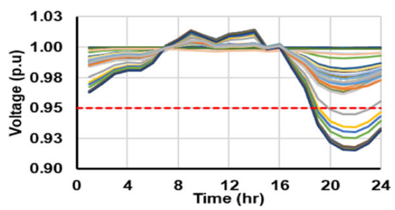

FIGURE 25 Voltage profile of IEEE 69 bus during 24 h with photovoltaic.

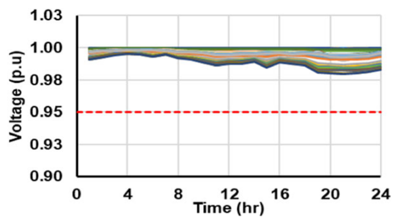

FIGURE 26 Voltage profile of IEEE 69 bus during 24 h with photovoltaic + battery energy storage.

displayed in Figure 20. The figure shows the power of the CQOBMO_7 in reaching the optimal solution.

A considerable improvement in the voltage profile is accomplished when installing DGs in the IEEE 69 bus system, as presented in Figure 21. Furthermore, that approving the importance of the optimal settlement of the DG in the distribution systems.

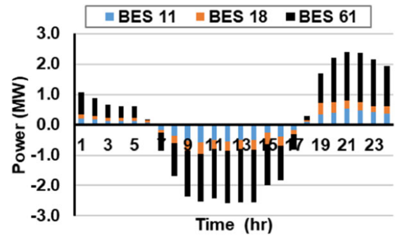

FIGURE 27 Charging/discharging powers of different BES integration in IEEE 69 bus. BES, battery energy storage.

TABLE 16 The optimal size of PV + BES in the IEEE 69-bus system.

Location	PV size (MW)	BES rated power (MW)	BES capacity (MW h)
Bus 11	0.88	0.57	4.55
Bus 18	0.62	0.40	3.05
Bus 61	2.72	1.77	14.63

Abbreviations: BES, battery energy storage; PV, photovoltaic.

TABLE 17 Daily energy losses for IEEE 69-bus.

Case	Energy losses (kW h)	Reduction %
Without PV	1822.33	-
With PV	1417.30	22.23
With PV + BES	586.87	67.80

Abbreviations: BES, battery energy storage; PV, photovoltaic.

(b) The optimal size of PV + BES using improved BMO
Similarly, the impact of the PV and the PV + BES is observed in the IEEE 69-bus system. Three PV units with different power generation are installed at the optimal locations, as shown in Figure 22. The performance of the IEEE 69-bus is improved by using the optimal power generation based on PV + BES, and that is clear in Figure 23. The figure shows that the power loss is significantly decreased in the case of PV + BES compared to the base case and when PV is installed.
In addition, the voltage profile is improved in the case of PV + BES (see Figure 26) compared to the base case and PV (see Figures 24 and 25), which shows the merits of installing BES with the PV systems.
Figure 27 presents the behavior of the BES at a different location during the 24 h. The BESs start discharging when the PV power is low, and they charge when the PV power is high to minimize the power loss.
The optimal sizes of the PV + BES for the IEEE 69-bus system are given in Table 16, and the

reduction in the energy is summarized in Table 17. The table shows that a significant energy reduction is achieved in the case of PV + BES, which reaches 67.80%.

6 | CONCLUSION

In this paper, improved versions of a new bioinspired optimization algorithm called BMO have been proposed for the optimal allocation and scheduling of the PVDG and BES in RDS. The conventional BMO has been improved using two improvement methods; the first method used a quasi oppositional of the search agents to increase the search space within the variable limits. The second method used the chaotic maps to improve the exploration phase of the improved QOBMO. The improved methods have been validated using 23 benchmarks, which proved the efficiency of the improved methods in achieving the optimal solution for the unimodal, multimodal, and composite functions. Parametric and non-parametric statistical analyses have been performed to measure the performance of the improved methods. Then, the improved methods have been applied for optimal PVDG allocation in the distribution power system using two standard IEEE 33-bus and IEEE 69-bus systems. A comparison between the improved methods and other optimization algorithms has been performed, and the results showed their effectiveness. In addition, the intermittent nature of DG has been studied using PVDG, considering the load variation for 24 h. Suitable scheduling of PVDG + BES using the improved CQOBMO has been achieved to solve the variation in the PV power generation; The results show that significant reductions have been achieved in the energy loss reaching 64% and 67.80% in IEEE 33-bus and 69-bus, respectively, when integrating PVDG + BES. In future work, further DG-based renewable energy resources such as wind could be modeled using uncertainty and optimally allocated in the RDSs. Besides this, long-term analysis considering both capital and operational expenditure of the PV and BES system will be optimized.

ACKNOWLEDGMENTS

The authors thank the support of the Science and Technology Development Fund (STDF), Egypt and the Ministry of Science and Technology (MOST), China, project No. 43180 "Chinese-Egytian Research Fund" (CERF), for providing partial research funding to the work reported in this research.

CONFLICTS OF INTEREST

The authors declare no conflicts of interest.

ORCID

Salah Kamel http://orcid.org/0000-0001-9505-5386
Baseem Khan http://orcid.org/0000-0002-5082-8311
Francisco Jurado http://orcid.org/0000-0001-8122-7415

REFERENCES

1. Datta U, Kalam A, Shi J. Smart control of BESS in PV integrated EV charging station for reducing transformer overloading and providing battery-to-grid service. *J Energy Storage*. 2020;28:101224.
2. Lai LL, Chan TF. *Distributed Generation: Induction and Permanent Magnet Generators*. John Wiley & Sons; 2008.
3. Kamel S, Selim A, Ahmed W, Jurado F. Single-and multi-objective optimization for photovoltaic distributed generators implementation in probabilistic power flow algorithm. *Electr Eng*. 2020;102:331-347.
4. Selim A, Kamel S, Jurado F. Efficient optimization technique for multiple DG allocation in distribution networks. *Appl Soft Comput*. 2020;86:105938.
5. Selim A, Kamel S, Jurado F, Lopes JAP, Matos M. Optimal setting of PV and battery energy storage in radial distribution systems using multi-objective criteria with fuzzy logic decision-making. *IET Gener Transm Distrib*. 2021;15:135-148.
6. Luo L, Abdulkareem SS, Rezvani A, et al. Optimal scheduling of a renewable based microgrid considering photovoltaic system and battery energy storage under uncertainty. *J Energy Storage*. 2020;28:101306.
7. Thokar RA, Gupta N, Niazi K, Swarnkar A, Meena NK. Multiobjective nested optimization framework for simultaneous integration of multiple photovoltaic and battery energy storage systems in distribution networks. *J Energy Storage*. 2021;35:102263.
8. Jiang Y, Kang L, Liu Y. Multi-objective design optimization of a multi-type battery energy storage in photovoltaic systems. *J Energy Storage*. 2021;39:102604.
9. Sulaiman MH, Mustaffa Z, Saari MM, Daniyal H. Barnacles mating optimizer: a new bio-inspired algorithm for solving engineering optimization problems. *Eng Appl Artif Intell*. 2020;87:103330.
10. Zhao W, Wang L, Zhang Z. Artificial ecosystem-based optimization: a novel nature-inspired meta-heuristic algorithm. *Neural Comput Appl*. 2019;653:1-43.
11. Dutta T, Bhattacharyya S, Dey S, Platos J. Border Collie optimization. *IEEE Access*. 2020;8:109177-109197.
12. Yang X-S. *Nature-Inspired Metaheuristic Algorithms*. Luniver Press; 2010.
13. Mirjalili S, Lewis A. The whale optimization algorithm. *Adv Eng Software*. 2016;95:51-67.
14. Storn R, Price K. Differential evolution—a simple and efficient heuristic for global optimization over continuous spaces. *J Global Optimiz*. 1997;11(4):341-359.
15. Mitchell M. *An Introduction to Genetic Algorithms*. MIT Press; 1998.
16. Chen X, Liu Y, Li X, Wang Z, Wang S, Gao C. A new evolutionary multiobjective model for traveling salesman problem. *IEEE Access*. 2019;7:66964-66979.

17. Montiel O, Castillo O, Melin P, Díaz AR, Sepúlveda R. Human evolutionary model: A new approach to optimization. *Inf Sci*. 2007;177(10):2075-2098.
18. Simon D. Biogeography-based optimization. *IEEE Trans Evolut Computat*. 2008;12(6):702-713.
19. Kennedy J, Eberhart R. Particle swarm optimization. Proceedings of ICNN'95-International Conference on Neural Networks, Vol. 4; 1995:1942-1948. IEEE.
20. Mirjalili S. Moth-flame optimization algorithm: A novel nature-inspired heuristic paradigm. *Knowl-based Syst*. 2015;89: 228-249.
21. Cuevas E, Cienfuegos M. A new algorithm inspired in the behavior of the social-spider for constrained optimization. *Expert Syst Appl*. 2014;41(2):412-425.
22. Mirjalili S, Mirjalili SM, Lewis A. Grey wolf optimizer. *Adv Eng Software*. 2014;69:46-61.
23. Karaboga D, Basturk B. A powerful and efficient algorithm for numerical function optimization: artificial bee colony (ABC) algorithm. *J Global Optimiz*. 2007;39(no. 3):459-471.
24. Saremi S, Mirjalili S, Lewis A. Grasshopper optimisation algorithm: theory and application. *Adv Eng Softw*. 2017;105:30-47.
25. Mirjalili S, Gandomi AH, Mirjalili SZ, Saremi S, Faris H, Mirjalili SM. Salp swarm algorithm: a bio-inspired optimizer for engineering design problems. *Adv Eng Softw*. 2017;114:163-191.
26. Heidari AA, Mirjalili S, Faris H, Aljarah I, Mafarja M, Chen H. Harris hawks optimization: algorithm and applications. *Future Gener Comput Syst*. 2019;97:849-872.
27. Ghasemi-Marzbali A. A novel nature-inspired meta-heuristic algorithm for optimization: bear smell search algorithm. *Soft Comput*. 2020;24(17):13003-13035.
28. Das AK, Pratihar DK. A new bonobo optimizer (BO) for real-parameter optimization. 2019 IEEE Region 10 Symposium (TENSYMP); 2019:108-113: IEEE.
29. Wang G-G. Moth search algorithm: a bio-inspired metaheuristic algorithm for global optimization problems. *Memetic Comput*. 2018;10(2):151-164.
30. Yang Y, Chen H, Heidari AA, Gandomi AH. Hunger games search: visions, conception, implementation, deep analysis, perspectives, and towards performance shifts. *Expert Syst Appl*. 2021;177:114864.
31. Tu J, Chen H, Wang M, Gandomi AH. The colony predation algorithm. *J Bionic Eng*. 2021;18(3):674-710.
32. Wang G-G, Deb S, Cui Z. Monarch butterfly optimization. *Neural Comput Appl*. 2019;31(7):1995-2014.
33. Zhao W, Wang L, Zhang Z. Atom search optimization and its application to solve a hydrogeologic parameter estimation problem. *Knowl-Based Syst*. 2019;163:283-304.
34. Kirkpatrick S, Gelatt CD, Vecchi MP. Optimization by simulated annealing. *Science*. 1983;220(4598):671-680.
35. Eskandar H, Sadollah A, Bahreininejad A, Hamdi M. Water cycle algorithm—a novel metaheuristic optimization method for solving constrained engineering optimization problems. *Comput Struct*. 2012;110:151-166.
36. Webster B, Bernhard PJ. A local search optimization algorithm based on natural principles of gravitation. Proceedings of the International Conference on Information and Knowledge Engineering. IKE'03; 2003.
37. Kaveh A, Bakhshpoori T. Water evaporation optimization: a novel physically inspired optimization algorithm. *Comput Struct*. 2016;167:69-85.
38. Shareef H, Ibrahim AA, Mutlag AH. Lightning search algorithm. *Appl Soft Comput*. 2015;36:315-333.
39. Faramarzi A, Heidarinejad M, Stephens B, Mirjalili S. Equilibrium optimizer: a novel optimization algorithm. *Knowl-Based Syst*. 2020;191:105190.
40. Li S, Chen H, Wang M, Heidari AA, Mirjalili S. Slime mould algorithm: a new method for stochastic optimization. *Future Gener Comput Syst*. 2020;111:300-323.
41. Bouchekara H. Most valuable player algorithm: a novel optimization algorithm inspired from sport. *Operat Res*. 2017: 1-57.
42. Zhang LM, Dahlmann C, Zhang Y. Human-inspired algorithms for continuous function optimization. 2009 IEEE international conference on intelligent computing and intelligent systems, vol. 1; 2009:318-321. IEEE.
43. Rao RV, Savsani VJ, Vakharia D. Teaching–learning-based optimization: an optimization method for continuous non-linear large scale problems. *Inf Sci*. 2012;183(1):1-15.
44. Satapathy S, Naik A. Social group optimization (SGO): a new population evolutionary optimization technique. *Compl Intell Syst*. 2016;2(3):173-203.
45. Kashan AH. League Championship Algorithm (LCA): an algorithm for global optimization inspired by sport championships. *Appl Soft Comput*. 2014;16:171-200.
46. Mohamed AW, Hadi AA, Mohamed AK, Cybernetics. Gaining-sharing knowledge based algorithm for solving optimization problems: a novel nature-inspired algorithm. *Int J Mach Learning*. 2020;11(7):1501-1529.
47. Ahmadianfar I, Heidari AA, Gandomi AH, Chu X, Chen H. RUN beyond the metaphor: an efficient optimization algorithm based on Runge Kutta method. *Expert Syst Appl*. 2021; 181:115079.
48. Rao R. Rao algorithms: three metaphor-less simple algorithms for solving optimization problems. *Int J Indust Eng Computat*. 2020;11(1):107-130.
49. Ahmadianfar I, Heidari AA, Noshadian S, Chen H, Gandomi AH. INFO: an efficient optimization algorithm based on weighted mean of Vectors. *Expert Syst Appl*. 2022; 195:116516.
50. Wolpert DH, Macready WG. No free lunch theorems for optimization. *IEEE Trans Evolut Comput*. 1997;1(1):67-82.
51. Pecora LM, Carroll TL. Synchronization in chaotic systems. *Phys Rev Lett*. 1990;64(8):821-824.
52. Emary E, Zawbaa HM. Impact of chaos functions on modern swarm optimizers. *PLoS One*. 2016;11(7):e0158738.
53. Li-Jiang Y, Tian-Lun C. Application of chaos in genetic algorithms. *Commun Theor Phys*. 2002;38(2):168-172.
54. Liu B, Wang L, Jin Y-H, Tang F, Huang D-X. Improved particle swarm optimization combined with chaos. *Chaos, Solitons Fractals*. 2005;25(5):1261-1271.
55. Zawbaa HM, Emary E, Grosan C. Feature selection via chaotic antlion optimization. *PLoS One*. 2016;11(3):e0150652.
56. Kaur G, Arora S. Chaotic whale optimization algorithm. *J Computat Design Eng*. 2018;5(3):275-284.
57. Kohli M, Arora S. Chaotic grey wolf optimization algorithm for constrained optimization problems. *J Computat Design Eng*. 2018;5(4):458-472.
58. Saremi S, Mirjalili S, Lewis A. Biogeography-based optimisation with chaos. *Neural Comput Appl*. 2014;25(5):1077-1097.

59. Menesy AS, Sultan HM, Selim A, Ashmawy MG, Kamel S. Developing and applying chaotic harris hawks optimization technique for extracting parameters of several proton exchange membrane fuel cell stacks. *IEEE Access*. 2019;8:1146-1159.
60. Tizhoosh HR. Opposition-based learning: a new scheme for machine intelligence. International Conference on Computational Intelligence for Modelling, Control and Automation and International Conference on Intelligent Agents, Web Technologies and Internet Commerce (CIMCA-IAWTIC'06), Vol. 1; 2005:695-701. IEEE.
61. Roy PK, Bhui S. Multi-objective quasi-oppositional teaching learning based optimization for economic emission load dispatch problem. *Int J Electr Power Energy Syst*. 2013;53:937-948.
62. Sultana S, Roy PK. Multi-objective quasi-oppositional teaching learning based optimization for optimal location of distributed generator in radial distribution systems. *Int J Electr Power Energy Syst*. 2014;63:534-545.
63. Sharma S, Bhattacharjee S, Bhattacharya A. Quasi-oppositional swine influenza model based optimization with quarantine for optimal allocation of DG in radial distribution network. *Int J Electr Power Energy Syst*. 2016;74:348-373.
64. Yu J, Kim C-H, Rhee S-B. Oppositional Jaya algorithm with distance-adaptive coefficient in solving directional over current relays coordination problem. *IEEE Access*. 2019;7:150729-150742.
65. Lian J, Zhang Y, Ma C, Yang Y, Chaima E. A review on recent sizing methodologies of hybrid renewable energy systems. *Energy Convers Manage*. 2019;199:112027.
66. Mingxue L, Guolai Y, Xiaoqing L, Guixiang B. Variable universe fuzzy control of adjustable hydraulic torque converter based on multi-population genetic algorithm. *IEEE Access*. 2019;7:29236-29244.
67. Abou El-Ela AA, El-Seheimy RA, Shaheen AM, Wahbi WA, Mouwafi MT. PV and battery energy storage integration in distribution networks using equilibrium algorithm. *J Energy Storage*. 2021;42:103041.
68. Kansal S, Kumar V, Tyagi B. Hybrid approach for optimal placement of multiple DGs of multiple types in distribution networks. *Int J Electr Power Energy Syst*. 2016;75:226-235.
69. Hung DQ, Mithulananthan N. Multiple distributed generator placement in primary distribution networks for loss reduction. *IEEE Trans Ind Electron*. 2013;60(no. 4):1700-1708.
70. Ehsan A, Yang Q. Optimal integration and planning of renewable distributed generation in the power distribution networks: a review of analytical techniques. *Appl Energy*. 2018;210:44-59.
71. Moradi MH, Abedinie M, Tolabi HB. Optimal multi-distributed generation location and capacity by genetic algorithms. 2010 Conference Proceedings IPEC; 2010:614-618. IEEE.
72. El-Zonkoly A. Optimal placement of multi-distributed generation units including different load models using particle swarm optimization. *Swarm Evol Computat*. 2011;1(1):50-59.
73. Celli G, Ghiani E, Mocci S, Pilo F. A multiobjective evolutionary algorithm for the sizing and siting of distributed generation. *IEEE Trans Power Syst*. 2005;20(2):750-757.
74. Lalitha MP, Reddy VV, Reddy NS, Reddy VU. DG source allocation by fuzzy and clonal selection algorithm for minimum loss in distribution system. *Distrib Gener Altern Energy J*. 2011;26(4):17-35.
75. El-Fergany A. Optimal allocation of multi-type distributed generators using backtracking search optimization algorithm. *Int J Electr Power Energy Syst*. 2015;64:1197-1205.
76. Devabalaji K, Ravi K. Optimal size and siting of multiple DG and DSTATCOM in radial distribution system using Bacterial Foraging Optimization Algorithm. *Ain Shams Eng J*. 2016;7(3):959-971.
77. ChithraDevi S, Lakshminarasimman L, Balamurugan R. Stud Krill herd Algorithm for multiple DG placement and sizing in a radial distribution system. *Eng Sci Technol Int J*. 2017;20(2):748-759.
78. Reddy PDP, Reddy VV, Manohar TG. Whale optimization algorithm for optimal sizing of renewable resources for loss reduction in distribution systems. *Renew Wind Water Solar*. 2017;4(1):3.
79. Atwa Y, El-Saadany E, Salama M, Seethapathy R. Optimal renewable resources mix for distribution system energy loss minimization. *IEEE Trans Power Syst*. 2010;25(1):360-370.
80. Hung DQ, Mithulananthan N, Lee KY. Determining PV penetration for distribution systems with time-varying load models. *IEEE Trans Power Syst*. 2014;29(6):3048-3057.
81. Derrac J, García S, Molina D, Herrera F. A practical tutorial on the use of nonparametric statistical tests as a methodology for comparing evolutionary and swarm intelligence algorithms. *Swarm Evol Computat*. 2011;1(1):3-18.
82. Baran ME, Wu FF. Network reconfiguration in distribution systems for loss reduction and load balancing. *IEEE Trans Power Delivery*. 1989;4(2):1401-1407.
83. Sultana S, Roy PK. Multi-objective quasi-oppositional teaching learning based optimization for optimal location of distributed generator in radial distribution systems. *Int J Electr Power Energy Syst*. 2014;63:534-545.
84. Baran M, Wu FF. Optimal sizing of capacitors placed on a radial distribution system. *IEEE Trans Power Delivery*. 1989;4(1):735-743.

How to cite this article: Selim A, Kamel S, Zawbaa HM, Khan B, Jurado F. Optimal allocation of distributed generation with the presence of photovoltaic and battery energy storage system using improved barnacles mating optimizer. *Energy Sci Eng*. 2022;10:2970-3000. doi:10.1002/ese3.1182